THE JOURNAL OF BIOLOGICAL CHEMISTRY VOL. 289, NO. 25, pp. 17350–17364, June 20, 2014

The Splicing Factor FUBP1 Is Required for the Efficient Splicing of Oncogene *MDM2* Pre-mRNA*[S]

Received for publication, February 6, 2014, and in revised form, April 25, 2014 Published, JBC Papers in Press, May 5, 2014, DOI 10.1074/jbc.M114.554717

Aishwarya G. Jacob[‡§¶], Ravi K. Singh[‡§], Fuad Mohammad[‡¶], Thomas W. Bebee[‡§], and Dawn S. Chandler[‡§¶1]

From the [‡]Center for Childhood Cancer, Research Institute at Nationwide Children's Hospital, Columbus, Ohio 43205 and the [§]Department of Pediatrics, Molecular, Cellular and Developmental Biology Program, and [¶]Center for RNA Biology, Wexner Medical Center, The Ohio State University, Columbus, Ohio 43210

Background: *MDM2* is alternatively spliced into shorter isoforms under DNA damage and in several cancers through unknown mechanisms.
Results: FUBP1 inactivation decreases splicing efficiency of an *MDM2* minigene and causes exon skipping of endogenous *MDM2* under normal conditions. Its overexpression attenuates damage-induced skipping of *MDM2* exons.
Conclusion: FUBP1 positively regulates efficient *MDM2* splicing.
Significance: This work uncovers an important mechanism regulating splicing efficiency of the oncogene *MDM2*.

Alternative splicing of the oncogene *MDM2* is a phenomenon that occurs in cells in response to genotoxic stress and is also a hallmark of several cancer types with important implications in carcinogenesis. However, the mechanisms regulating this splicing event remain unclear. Previously, we uncovered the importance of intron 11 in *MDM2* that affects the splicing of a damage-responsive *MDM2* minigene. Here, we have identified discrete *cis* regulatory elements within intron 11 and report the binding of FUBP1 (Far Upstream element-Binding Protein 1) to these elements and the role it plays in *MDM2* splicing. Best known for its oncogenic role as a transcription factor in the context of c-*MYC*, FUBP1 was recently described as a splicing regulator with splicing repressive functions. In the case of *MDM2*, we describe FUBP1 as a positive splicing regulatory factor. We observed that blocking the function of FUBP1 in *in vitro* splicing reactions caused a decrease in splicing efficiency of the introns of the *MDM2* minigene. Moreover, knockdown of FUBP1 in cells induced the formation of *MDM2-ALT1*, a stress-induced splice variant of *MDM2*, even under normal conditions. These results indicate that FUBP1 is also a strong positive splicing regulator that facilitates efficient splicing of the *MDM2* pre-mRNA by binding its introns. These findings are the first report describing the regulation of alternative splicing of *MDM2* mediated by the oncogenic factor FUBP1.

MDM2 (Murine Double Minute 2) is an oncogenic protein that functions chiefly through the negative regulation of the tumor suppressor p53 (1–3). The amplification and overexpression of full-length MDM2 have been implicated in the etiology of various types of cancer (4, 5). Alternative splicing of *MDM2* resulting in truncated isoforms incapable of regulating p53 has also been reported as a hallmark of several tumor types (6–14). One such splice variant is *MDM2-ALT1*, a form that lacks all internal exons and includes only the terminal coding exons (exons 3 and 12) of *MDM2*. The impact of *MDM2* splice variants on cancer is evidenced by their association with aggressive, high grade tumors (8, 10, 11, 14). We recently showed, in a panel of pediatric rhabdomyosarcoma tumors, >90% of the metastatic tumors were positive for *MDM2-ALT1* (15). Furthermore, MDM2-ALT1 and MDM2-ALT2 (another *MDM2* splice variant frequently observed in tumors) have been shown to accelerate tumorigenesis in *in vitro* and *in vivo* studies (15–19). Indeed, a recent study showed that the expression of splice variant MDM2-ALT1 in colorectal cancer cells considerably increased the tumorigenic properties of these cells by causing the accumulation of mutant p53 (gain-of-function p53 mutants) (19). It is therefore important to understand the mechanisms regulating the alternative splicing of *MDM2* in cancer.

Another important context in which the alternative splicing of *MDM2* is observed is in the response of cells to genotoxic stress. Treatment with DNA-damaging agents such as UV irradiation and cisplatinum induces the formation of *MDM2-ALT1* transcripts (20, 21). We have utilized this inducible system to develop an *in vitro* splicing assay using nuclear extracts from normal and cisplatinum-treated HeLa S3 cells and a damage-responsive *MDM2* minigene. Using this *in vitro* splicing assay, we previously reported the importance of evolutionarily conserved regions in intron 11 of *MDM2* for the normal and damage-induced splicing of the *MDM2* minigene (22). In this study, we have narrowed down specific *cis* elements within intron 11 that influence the regulation of damage-inducible exon 11 skipping of the *MDM2* minigene. Furthermore, we have identified potential regulators of the alternative splicing of *MDM2* by isolating the *trans* protein factors that exhibited differential binding at these intron 11 *cis* elements under normal and cisplatinum-damaged conditions. We identified FUBP1 (Far Upstream element-Binding Protein 1) as one such protein.

FUBP1 is considered a proto-oncogene and is a biomarker for a variety of cancer types in which it is highly expressed,

* This work was supported, in whole or in part, by National Institutes of Health Grant 1R01CA133571 (to D. S. C.).
[S] This article contains supplemental Table S1.
[1] To whom the correspondence should be addressed: The Center for Childhood Cancer, The Research Institute at Nationwide Children's Hospital, Rm. WA5023, 700 Children's Dr., Columbus, OH 43205-2696. Tel.: 614-722-5598; Fax: 614-722-5895; E-mail: Dawn.Chandler@nationwidechildrens.org.

including hepatocellular carcinoma, non-small cell lung carcinoma, gliomas, and gastric cancer (23–28). However, in oligodendrogliomas, where its expression is abolished due to mutations, *FUBP1* is considered a tumor suppressor (28–30). Functionally, FUBP1 is a DNA helicase V (31) and is best known for its role in the transcriptional up-regulation of c-*MYC* through its binding of single-stranded DNA at the far upstream element (32) via the four tandem K homology motifs in its central domain (33, 34). However, it is capable of binding single-stranded RNA and post-transcriptional functions have been described for FUBP1 in mRNA turnover and translation control (35–38). Although a close family member FUBP2 (KHSRP) is a known splicing regulator (39), FUBP1 itself had previously not been implicated in splicing despite the fact that its presence had been identified in the spliceosomal complex (40). It was only recently that evidence describing a splicing regulatory role for FUBP1 emerged in which FUBP1 has been demonstrated to function as a suppressor of the second step of splicing through its binding of a 30-nt[2] AU-rich exonic splicing silencer element on the *triadin* exon 10 in a chimeric minigene context (41). In contrast, in this study, we describe FUBP1 as a positive splicing regulator of the oncogene *MDM2*. We show here the binding of endogenous FUBP1 to intronic splicing enhancer elements in intron 11 of *MDM2* and the role it plays in enhancing the efficient splicing of full-length *MDM2*, thus making this the second report to identify a splicing regulatory role for FUBP1 and the first report to describe an enhancer role for this splicing regulator.

EXPERIMENTAL PROCEDURES

Cell Lines and Culture Conditions—HeLa (cervical cancer) and MCF7 (breast cancer) cells were cultured under standard conditions using DMEM with high glucose and supplemented with 10% FBS (Hyclone, Logan, UT), L-glutamine (Cellgro, 25-005 CI), and penicillin/streptomycin (Cellgro, 30-001 CI). HeLa S3 cells were maintained in RPMI 1640 medium supplemented with 10% FBS, L-glutamine, and penicillin/streptomycin. For nuclear extract preparation, HeLa S3 cells were cultured in spinner flasks (Bellco, Vineland, NJ) with slow rotation of 90 rpm. For the phosphatase assays, 30 μg of normal or cisplatinum-damaged HeLa nuclear extracts were incubated for 1 h at 37 °C with 12 units of CIP (Ipswich, MA) and then loaded onto an SDS-polyacrylamide gel. For the caspase inhibitor experiments HeLa S3, cells were incubated in pan-caspase inhibitor Boc-Asp (OMe)-fluoromethyl ketone (BAF, catalog no. B2682, Sigma; a kind gift from Dr. Katsumi Kitagawa, Nationwide Children's Hospital, Columbus, OH) at a concentration of 50 μM or an equal volume of DMSO for 1 h. Cells were then treated with 75 μM cisplatinum for 12 h or left untreated. Cells were then harvested for protein and analyzed using Western blotting.

Nuclear Cytoplasmic Fractionation of HeLa S3 Cells—The cells were cultured on plates in RPMI 1640 media under standard conditions. They were then treated with cisplatinum (75 μM) or left untreated for 12 h after which they were trypsinized and spun down at 1000 rpm for 10 min in a clinical centrifuge. About 1/10th of the cells were removed and resuspended in RIPA buffer to obtain the whole-cell extract. The remaining cells were washed and resuspended in hypotonic buffer A (10 mM HEPES-KOH, pH 8.0, 10 mM KCl, 1.5 mM $MgCl_2$) and incubated on ice for 10 min. Following this, the cells were centrifuged, ruptured using a 26-gauge needle, and then centrifuged again at 2000 rpm for 10 min to separate the nuclei and the cytoplasmic extract. The nuclei were then washed again and resuspended in RIPA buffer to obtain the nuclear extract. 30 μg of protein from these fractions were subsequently used for immunoblotting.

HeLa S3 Nuclear Extract Preparations and in Vitro Splicing Assays—Normal and cisplatinum-damaged HeLa S3 nuclear extracts were prepared as described previously (22). Briefly, HeLa S3 cells were cultured under either normal or cisplatinum-treated conditions, and cells were harvested when in log phase of growth, and nuclear extracts were prepared using standard protocols (42, 43). Cisplatinum (APP Pharmaceuticals LLC, Schaumberg, IL) treatment was for 12 h at a concentration of 75 μM. Immunointerference *in vitro* splicing assays were performed in normal nuclear extracts using either anti-FUBP1 antibody (sc-48821 clone H-42) or control rabbit IgG (0111-01, Southern Biotech, Birmingham, AL). These *in vitro* splicing reactions were carried out at 30 °C, as described previously (22), with the difference that the nuclear extracts were incubated with 0.5 μg/reaction of either anti-FUBP1 or the isotype control antibody for 45 min prior to splicing. 20 fmol of cold *in vitro* transcribed pre-mRNA (T7 MEGAscript, Ambion, Austin, TX) was used as splicing substrate. Products of the splicing reactions were isolated after 2 h of splicing and reverse-transcribed using gene-specific primers. The cDNA was then used in a PCR to amplify the linear products of splicing using 5′-end-labeled γ-^{32}P-FLAG tag forward primer and the gene-specific reverse primers. The reverse primers and the PCR conditions (18 or 25 cycles) used for amplification of splicing products from the *MDM2* and the *p53* minigenes are as follows: for *MDM2* exon 11, 5′-ACTTACAGCTAAGGAAATTTCAGGATCTTC-3′; for *MDM2* exon 12, 5′-ACTTACGGCCCAACATCTGTTGCAATGTGATGG-3′; for *p53* exon 8, 5′-ACTTACCTCGCTTAGTGCTCCCTGGGGGCAGC-3′, and for *p53* exon 9, 5′-ACTTACGGCTGAAGGGTGAAATATTCTCCATCC-3′. The PCR products were then resolved on 6% sequencing gel (urea-PAGE), dried, exposed to a phosphorimager screen, and scanned using a Typhoon imager (GE Healthcare). The bands were quantified using ImageQuant (version 8.1). For the *MDM2* 3-exon immunointerference splicing experiments, splicing efficiency was calculated as the ratio of either full-length (3.11.12) or skipped (3.12) spliced product to the unspliced pre-mRNA. For the 2-exon *MDM2* and *p53* minigene systems, splicing efficiency was determined as the ratio of the spliced product to the unspliced pre-mRNA in every reaction. All experiments were conducted in at least three independent trials. Statistical analyses were performed using GraphPad Prism 6.0c. Two-tailed, unpaired *t* tests were used to evaluate the significance of the splicing changes under the various conditions, and the error bars were represented as S.E.

[2] The abbreviations used are: nt, nucleotide; BAF, Boc-Asp (OMe)-fluoromethyl ketone; CIP, calf intestinal phosphatase; TCGA, The Cancer Genome Atlas.

UVC Cross-linking Assay—To obtain transcripts pertaining to regions RNA1, -2, -3, -4, -A, and -B, specific primer pairs with T7 promoter overhang at the 5′-end of the forward primer were first used to amplify the corresponding regions of the *MDM2* minigene. The primer pairs used were as follows: RNA1 (142 bp), sense 5′-GGAATTCTAATACGACTCACTATAGGCAAGTTACTGTGTATCAGGC-3′ and antisense 5′-GCTAGATATAGTCTCCTAATC-3′; RNA2 (123 bp), sense 5′-GGAATTCTAATACGACTCACTATAGGGATTAGGAGACTATATCTAGC-3′ and antisense 5′-CAGCATGAGGACTATAGTTAG-3′; RNA3 (135 bp), sense 5′-GGAATTCTAATACGACTCACTATAGGTTAGTAAATTTCCAGTATACC-3′ and antisense 5′-GCAACTTTGCTATGTCTAAGG-3′; RNA4 (143 bp), sense 5′-GGAATTCTAATACGACTCACTATAGGTGAAACACTGAATATTGAGCC-3′ and antisense 5′-GAAGTGCATTTCCAATAGTCC-3′; RNA A (128 bp), sense 5′-GGAATTCTAATACGACTCACTATAGGGTAACCACCTCACAGATTCCAGC-3′ and antisense 5′-AGGCTACAATTGAGGTATACG-3′; and RNA B (118 bp), sense 5′-GGAATTCTAATACGACTCACTATAGGTAGGACTTATTACTAGGAAGCC-3′ and antisense 5′-GTATCACTCTCCCCTGCC-3′. These PCR products were then used as templates for *in vitro* transcription reactions (T7 MAXIscript kit, Ambion), and the radioactively labeled transcripts (internally labeled with [α-^{32}P]UTP) were purified. The radiolabeled RNA was then incubated for 30 min under splicing conditions (30 °C, 20 mM HEPES buffer, pH 7.4, 0.5 mM ATP, 20 mM creatine phosphate, 3.2 mM $MgCl_2$, 2.6% polyvinyl alcohol, and 100 ng of yeast tRNA to minimize nonspecific protein binding) in normal or cisplatinum-damaged nuclear extracts. The reactions were then transferred to a 96-well round bottom dish on ice, and the cross-linking was performed using the Stratalinker with UVC (254 nm) for 10 min. The plates were placed at 2 cm from the UVC lamp. After cross-linking, the reactions were transferred to Eppendorf tubes where they were treated with 50 units of RNase A and 50 units of RNase T1 at 37 °C for 15 min. Following this, the reactions were stopped using the SDS-sample buffer, and the cross-linked proteins were separated using SDS-PAGE (12% separating gel). The gel was then dried, exposed to a phosphorimager screen, and scanned using the Typhoon scanner. The image was analyzed using the ImageQuant software (version 5.0, GE Healthcare).

RNA Affinity Chromatography—The templates for the transcription of RNA2 (Δ1 and Δ3) and RNA A were amplified from the *MDM2* minigene as described in the UV cross-linking assay. Biotin-labeled transcripts were then obtained from these templates using the T7 MEGAshortscript (Ambion, TX) and 10 μl of biotin labeling mix (Roche Diagnostics). The biotin-labeled RNA was gel-purified and quantified (UVC spectrometry), and 2 μg of the labeled transcripts were bound to 60 μl of 50% streptavidin-agarose bead slurry (Novagen, WI) for 1 h at 4 °C. Prior to binding the biotinylated transcripts, the streptavidin-conjugated beads were equilibrated by washing twice in 1 ml of buffer D (20 mM HEPES-KOH, pH 8.0, 100 mM KCl, 0.2 mM EDTA, 20% glycerol, 0.5 mM PMSF, and 1 mM DTT). After the binding reaction, the beads were washed twice in buffer D to remove any unbound RNA. Following this, 600 μg of nuclear extract either normal or damaged was added to the RNA bound to the beads, under splicing conditions similar to the UV cross-linking assay, and incubated for 1 h for 4 °C. The beads bearing the biotinylated RNA and the proteins to them were then washed three times in buffer D. Finally, resuspending the agarose beads in 1.5× SDS sample buffer and boiling the samples eluted the proteins that were bound to the beads. The eluted proteins were separated by SDS-PAGE, and the gels were stained with silver stain (SilverSNAP stain for mass spectrometry, Thermo Scientific, Waltham, MA), and the proteins were visualized. Protein bands appearing differentially between the nuclear extracts from normal and damage-treated cells were excised and sequenced via tandem mass spectrometry (at the Mass Spectrometry and Proteomics Facility, The Ohio State University). The binding of the proteins identified in the mass spectrometry screen were subsequently verified by RNA affinity chromatography of the respective RNA regions followed by Western blotting using antibodies specific to these proteins.

Immunoblotting—Typically, 30 μg of protein lysates (quantified using the Pierce BCA protein assay kit, Thermoscientific, Rockford, IL) were separated using SDS-PAGE (4% stacking and 10% separating gels) using standard techniques followed by immunoblotting with the specified antibodies. For the detection of endogenous FUBP1 in HeLa cell lysates, for the immunointerference in *in vitro* splicing assays, and for confirmation of binding to RNA2 Δ1 and RNA A in the RNA chromatography assays, the anti-FUBP1 H-42 clone (sc-48821; Santa Cruz Biotechnology) was used. As loading controls, β-actin (AC-15, A5441; Sigma) or GAPDH (14C10, catalog no. 2118; Cell Signaling) was used. To confirm overexpression of FLAG-tagged FUBP1 isoforms, anti-FLAG M2 (F3165; Sigma) was used, and the anti-MYC tag antibody 9E10 clone (sc-40; Santa Cruz Biotechnology) was used to detect the MYC-tagged negative control overexpression constructs (MYC-LacZ or MYC-GFP). To detect SRSF1 in the phosphatase treatment experiments, the anti-SRSF1 antibody (clone 103, catalog no. 32-4600; Invitrogen) was utilized.

Overexpression and Knockdown Assays—The splicing of the 3-11-12 *MDM2* minigene and the intron 11 deletion constructs was assessed by transiently transfecting MCF7 cells with FuGENE 6 (Roche Diagnostics) according to the manufacturer's instructions. The cells were exposed to 50 J/m^2 UVC 24 h post-transfection and were harvested for RNA 20 h post-treatment. For the overexpression assays testing the functions of FUBP1 and its isoforms, HeLa cells were cotransfected with the corresponding expression constructs or a negative control (MYC-LacZ or MYC-GFP) and the *MDM2* 3-4-10-11-12 minigene using Lipofectamine 2000 (Invitrogen) according to the manufacturer's instructions. In this case, the cells were transfected at about 70% confluence on 10 cm plates. 18 h post-transfection, the cells were split into two groups for untreated and cisplatinum-treated conditions. At 24 h post-transfection, cisplatinum (APP Pharmaceuticals LLC, Schaumberg, IL, or Teva Pharmaceuticals, Irvine, CA) was added to the cells at a concentration of 75 μM. 24 h after treatment, both floating and adherent cells were collected and pooled, and RNA and protein were harvested from these cells. RNA was extracted using the RNeasy mini protocol (Qiagen, Valencia CA), and protein was extracted by resuspending the cells in RIPA buffer. For the

FUBP1 knockdown assays, HeLa cells were transfected with nonspecific siRNA or siFUBP1 using Lipofectamine 2000. 48 h post-transfection, cells were treated with cisplatinum for 24 h at and harvested (total of 72 h siRNA treatment) in a procedure similar to the overexpression assays. The siRNA sequences used were nonspecific (AAGGUCCGGCUCCCCCAAAUG) (44) and siFUBP1 (GGAGGAGUUAACGACGCUUUU) (41).

Protein Expression and Minigene Plasmid Constructs—The construction and cloning of the 3-11-12 and the 3-4-10-11-12 *MDM2* and the *p53* 7-8-9 minigenes into the pCMV-Tag2B vector (Stratagene, La Jolla, CA) have been described previously (22). Intron 11 deletions Δ1, Δ2, and Δ3 were first engineered into the 3-11-12 *MDM2* minigene, and these constructs were transfected into MCF7 cells to assess their splicing patterns and were also used to obtain templates for *in vitro* transcription of RNA2 Δ1, Δ2, and Δ3. Briefly, intron 11 with the corresponding deletions and exon 12 were amplified using primers containing EcoRI and XhoI restriction sites. The PCR products thus amplified were then digested with EcoRI and XhoI and used to replace these regions in the original *MDM2* 3-11-12 minigene. For the overexpression assays, *FUBP1* cDNA cloned into the pCDNA3.1 V5-FLAG vector was used. This plasmid was a kind gift from Dr. Sharon Dent (MD Anderson Cancer Center, Houston, TX). The Δ74 form of FUBP1 was constructed as described by Jang *et al.* (45) by amplifying the corresponding region of the *FUBP1* cDNA downstream of the caspase cleavage site (sense 5′-AGCACAGTGGCGGCCGCGCTAAGAAAGTTGCTCCTC-3′ and antisense 5′-GCCCTCTAGACTCGAGCTACAGAGCTAGTTCTATAC-3′) and cloning it into the NotI-XhoI sites of the pCDNA3.1-V5-FLAG vector (kind gift from Dr. Sharon Dent). The cloning was performed using the infusion kit (Clontech) according to manufacturer's instructions. All clones were verified by sequencing. The AQPA form was created by mutating the cleavage site of FUBP1 using the primers as described by Jang *et al.* (45) (sense 5′-GGAGCTCAACCAGCTGCTAAGAAAG-3′ and antisense 5′-CTTTCTTAGCAGCTGGTTGAGCTCC-3′) using the QuikChange II mutagenesis kit (Agilent, Santa Clara, CA). As negative control, MYC-tagged BNN-pCall2-LacZ (described in Jacob *et al.* (15) or MYC-GFP (pCS2* mt-SGP; a kind gift from Dr. Heithem El-Hodiri, The Ohio State University) was utilized.

Reverse Transcription and PCRs—Typically, 0.5–4 μg of total RNA was used for the reverse transcription reactions with random hexamers. Transcriptor RT enzyme (catalog no. 03531287001) from Roche Diagnostics was used for the cDNA synthesis reactions according to the manufacturer's instructions. PCRs were performed under standard conditions using *Taq* polymerase from Sigma (catalog no. D6677). For the amplification of the spliced products of the 3-4-10-11-12 *MDM2* minigene used in the FUBP1 overexpression assays, a combination of FLAG tag as the forward primer and a gene-specific reverse primer was used (5′-CAATCAGGAACATCAAAGCC-3′). The splicing of the *MDM2* 3-11-12 wild-type minigene and intron 11 deletion mutants was also assayed similarly using the reverse primer GGCCCAACATCTGTTGCAATGTGATGG. The PCRs were performed at a T_m of 55 °C for 35 cycles. The PCR products were resolved on a 1.5% agarose gel, and the relative quantities of the full-length spliced product (3.4.10.11.12) and *MDM2-ALT1* (3.12) were determined using ImageQuant (version 8.1) software. To detect endogenous *MDM2* transcripts, a nested PCR approach was utilized. An initial PCR (T_m of 62 °C, 35 cycles) was performed using external primers 5′-GAAGGAAACTGGGGAGTCT-3′ (sense) and 5′-GAGTTGGTGTAAAGGATG-3′(antisense). Following this, a second PCR (T_m of 55 °C, 35 cycles) was performed using a 1:10 dilution of the products of the first PCR as substrate for the second reaction with nested primers 5′-CAGGCAAATGTGCAATACCAAC-3′ (sense) and 5′-CAATCAGGAACATCAAAGC-3′ (antisense). The PCR products were resolved on a 1.5% agarose gel and quantified as mentioned previously.

TCGA Data Mining—The Cancer Genome Atlas (TCGA) data were accessed via the cBioportal for Cancer Genomics (46, 47) in April, 2014. *FUBP1* gene alterations were queried across all cancer studies in the portal. Kaplan-Meier curves generated for specific cancer types in response to the queried gene were also downloaded in April, 2014.

RESULTS

Intron 11 of Stress-responsive MDM2 Minigene Shows Differential Binding of Factors under Stress—We have previously shown that *MDM2* is alternatively spliced in response to genotoxic stress such as UV and cisplatinum treatment (20). Furthermore, we have demonstrated the damage-responsive alternative splicing of an *MDM2* minigene using an *in vitro* cell-free splicing assay with nuclear extracts from untreated and cisplatinum-treated (damaged) HeLa S3 cells (22). Moreover, using this minigene we showed that intron 11 of *MDM2* contains conserved elements (in a region spanning 73 nt near the 5′ splice site and 243 nt near the 3′ splice site) that are important for its stress-induced alternative splicing (22). We hypothesized that the differential splicing of the *MDM2* minigene in nuclear extracts from normal and damage-treated cells is the result of differential binding of *trans* regulatory splicing factors to *cis* regulatory elements within the conserved region of intron 11, and in this study we endeavored to define these elements and the proteins that bind them. To this end, we performed a UV cross-linking assay in which radioactively labeled transcripts spanning regions across the *MDM2* minigene's intron 11 (RNA1–4, Fig. 1*A*) were incubated in nuclear extracts from normal or damage-treated cells under splicing conditions, cross-linked with UVC irradiation (254 nm for 10 min), subjected to RNase digestion targeting unbound RNA, and then run on an SDS-polyacrylamide gel (Fig. 1*B*). Only proteins cross-linked to the radiolabeled RNA are able to be visualized on the resulting autoradiogram. The differential migration of proteins between the nuclear extracts from normal and damage-treated cells suggests differential binding of proteins to the radioactively labeled transcripts under the two conditions. We observed that RNA2 on intron 11 of the *MDM2* minigene showed clear differential banding patterns between nuclear extracts from normal or damage-treated cells with notably strong signals of cross-linking at ~55 and 65 kDa (Fig. 1*B*). For instance, the 55-kDa cross-linking band was observed in the nuclear extract from normal cells but not in the nuclear extract from damage-treated cells. However, the protein factor running at ~65 kDa bound RNA2 in damage treatment but not

under normal conditions raising the possibility that this factor plays a negative role in *MDM2* splicing (Fig. 1*B*). Additionally, we observed differential binding of a 65-kDa factor on RNA3 indicating the possibility that a single protein is associated with more than one binding site within the intron 11 RNA. Aside from these factors, RNA1, -3, and -4 also showed differential bands between the nuclear extracts from normal and damage-treated cells that were migrating at other sizes. However, we chose to focus on RNA2 (123 nt), the region exhibiting the most differential binding of *trans* protein factors, for further analysis. We first confirmed the specificity of the factors that bound RNA2 differentially in nuclear extracts from normal or damage-treated cells. To do this, we generated sequential deletions Δ1, Δ2, and Δ3 in the RNA2 region (Fig. 2*A*) and performed UV cross-linking on these transcripts in the two nuclear extracts. We observed that the differential bands observed on RNA2 at ~65 and 55 kDa were retained in RNA2 Δ1 but were completely abolished in the largest deletion RNA2 Δ3 (Fig. 2*B*). RNA2 Δ2 transcripts, however, were still able to bind the 65-kDa factor, although they lost the ability to interact with the 55-kDa protein (Fig. 2*B*). This indicates specificity of the binding of these factors to elements lying in the RNA2 region. We then transfected the *MDM2* 3-11-12 minigenes containing the RNA2 deletions Δ1, Δ2, and Δ3 into MCF7 cells and assayed them for splicing either in the absence (−) or presence (+) of DNA damage. The deletion constructs showed increased skipping of exon 11 compared with the control wild-type minigene even in absence of damage treatment, and this difference was statistically significant (compare *lanes 3, 5,* and *7* with the control WT 3-11-12 minigene in *lane 1*, Fig. 2*C*). This indicates that sequential deletion of regions within RNA2 of intron 11 of the *MDM2* minigene resulted in the loss of splicing enhancer elements within this region that are essential for regulating the splicing of exon 11.

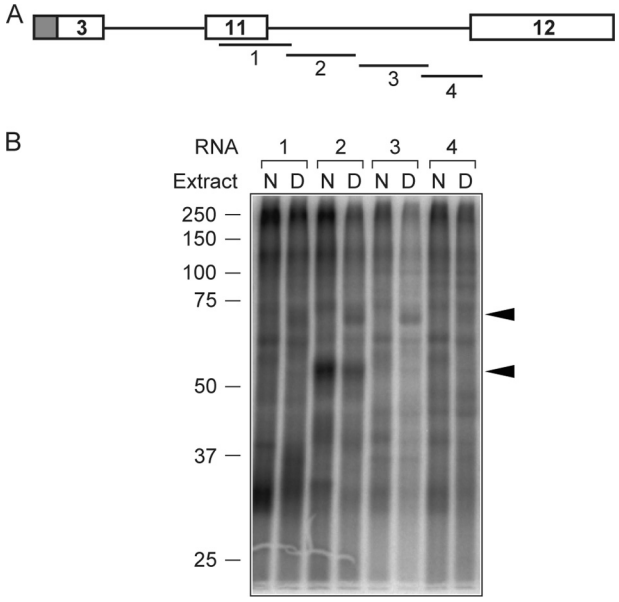

FIGURE 1. **UVC cross-linking assay reveals differential binding of proteins on intron 11 of *MDM2* between normal and damaged conditions.** *A,* intron 11 of the *MDM2* minigene was divided into four overlapping sections for examination of differential protein binding under normal (*N*) and cisplatinum-damaged (*D*) conditions. The regions are indicated as RNA1, -2, -3, and -4. *B,* UVC cross-linking of RNA1–4 shows the differential binding of proteins between normal and cisplatinum-damaged HeLa S3 nuclear extracts. RNA2 shows the most notable patterns of differential banding at ~55 and 65 kDa (indicated by *arrowheads*).

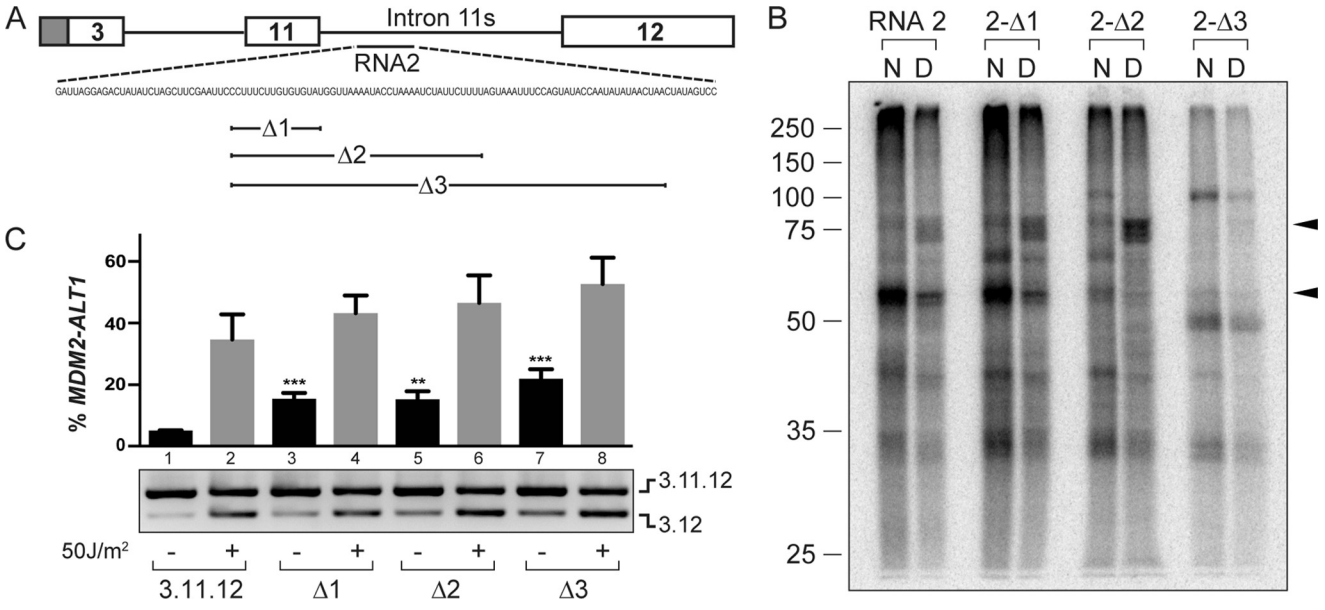

FIGURE 2. **Deletions within RNA2 result in loss of the binding of the differential protein factors and reduced exon 11 splicing.** *A, MDM2* minigene highlighting RNA2 and the sequential deletions Δ1, Δ2, and Δ3. *B,* UVC cross-linking of RNA2 Δ1, Δ2, and Δ3 shows the progressive loss of differential binding of factors between normal (*N*) and damaged (*D*) conditions with increasing size of deletion. The *arrowheads* indicate the cross-linking of bands at ~65 and 55 kDa. *C,* minigene constructs bearing the deletions in RNA2 region were transfected into MCF7 cells and subjected to UVC treatment (50 J/m^2). RNA was harvested, and RT-PCR was performed to assay the splicing of the wild-type and mutant *MDM2* minigenes. The deletions RNA2 Δ1, Δ2, and Δ3 show increased skipping of exon 11 compared with the wild-type minigene even in the absence of damage (compare *lanes 3, 5,* and *7* to the control *lane 1*). The percent *MDM2-ALT1 (3.12*) product from three independent experiments is graphically represented with S.E. (*error bars*). Two-tailed Student's *t* test indicates that the increase in *3.12* spliced product in the RNA2 Δ1, Δ2, and Δ3 constructs is statistically significant in comparison with the wild-type minigene. **, $p < 0.01$; ***, $p < 0.0001$.

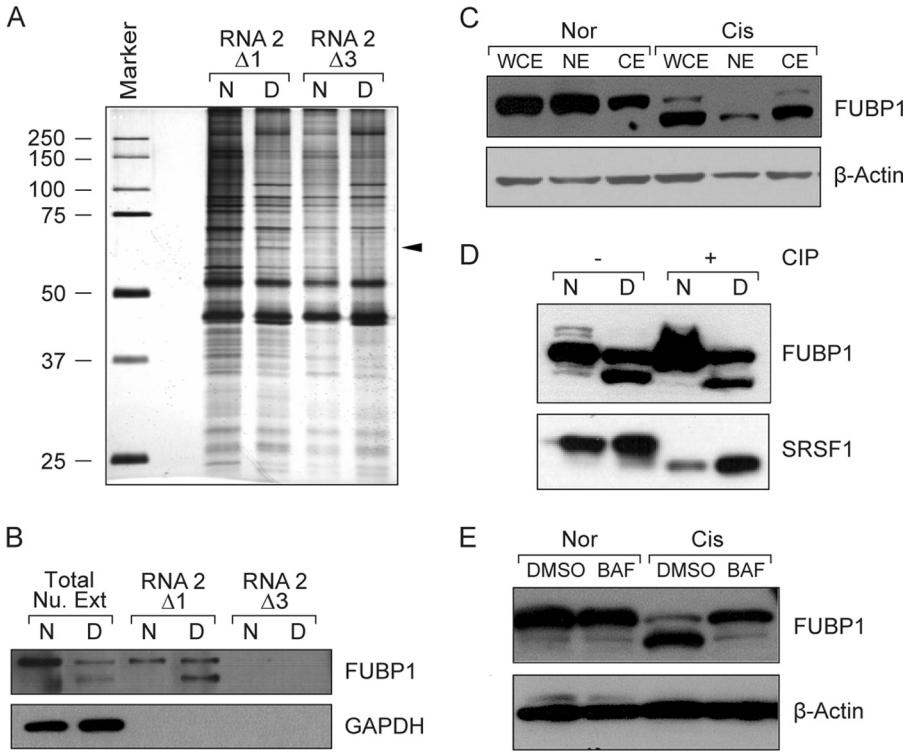

FIGURE 3. **FUBP1 and its damage-specific cleaved form bind RNA2.** *A,* RNA2 Δ1 and Δ3 regions were subjected to RNA affinity chromatography by incubating in normal (*N*) and damaged (*D*) nuclear extracts and then pulling down biotin-labeled RNA2 Δ1 and Δ3 transcripts. RNA2 Δ3 was used as a negative control to ensure the identification of specific protein factors. The proteins bound to these transcripts were isolated and subjected to SDS-PAGE followed by silver staining. The differential bands between normal and damaged conditions specific to RNA2 Δ1 were cut and subjected to tandem mass spectrometry, and the proteins were identified. The *arrow* indicates the differential band at ~65 kDa in nuclear extract from damage-treated cells. This band was identified as FUBP1 by the mass spectrometric analysis (supplemental Table S1). *B,* FUBP1 and a shorter isoform were identified as binding to RNA2 differentially between normal and damaged conditions. The binding was confirmed by RNA affinity chromatography of RNA2 Δ1 and Δ3 followed by Western blotting (anti-FUBP1, H-42). *C,* fractionation of HeLa S3 cells (untreated and cisplatinum-treated; 75 μM cisplatinum for 12 h) into whole-cell (*WCE*), nuclear (*NE*), and cytoplasmic (*CE*) extracts showed the appearance of the shorter isoform of FUBP1 in all three fractions of cisplatinum-treated cells. *D,* normal (*Nor*) and cisplatinum (*Cis*)-damaged HeLa S3 nuclear extracts were treated with CIP and then assessed for the presence of FUBP1 and the damage-specific short isoform. FUBP1 and its short form did not show differential migration between untreated (−) and CIP-treated (+) normal or cisplatinum-damaged nuclear extracts. As a positive control for CIP treatment, SRSF1, well known as a phosphoprotein, was examined for difference in migration patterns. CIP treatment of nuclear extracts caused SRSF1 to migrate faster on SDS-PAGE. *E,* HeLa S3 cells were incubated with the pan-caspase inhibitor BAF and then subjected to cisplatinum treatment for 12 h. Caspase inhibition prevented the appearance of the shorter isoform of FUBP1 under damage.

Mass Spectrometric Identification of Differentially Bound Proteins in Nuclear Extracts from Normal and Damage-treated Cells—To identify the specific factors that are differentially cross-linked to RNA2 in intron 11 of the *MDM2* minigene, we performed RNA affinity chromatography of biotin-labeled RNA2 Δ1 and Δ3 transcripts. RNA2 Δ1 is the minimal RNA that supports the binding of both the 55- and the 65-kDa proteins, whereas the RNA2 Δ3 transcripts served as the negative control because the specific binding of the proteins was abolished in the UV cross-linking studies. The labeled transcripts were incubated in nuclear extracts from normal or damage-treated cells under conditions that support pre-mRNA splicing, similar to the UV cross-linking experiment. Streptavidin-conjugated beads were then used to precipitate the biotin-labeled RNA and the proteins binding them. Following this, the bound proteins were dissociated from the beads and separated on an SDS-polyacrylamide gel and silver-stained (Fig. 3*A*). Bands specific to RNA2 Δ1 appearing differentially between the nuclear extracts from normal and damage-treated cells were excised from the gel, and the proteins therein were identified using tandem mass spectrometry (Fig. 3*A*; the gel highlights findings consistent in three independent experiments). Importantly, these bands did not appear in the RNA2 Δ3 pulldown lanes indicating specificity to the splicing regulatory regions within RNA2 Δ1. All proteins identified in the differential bands on RNA2 Δ1 and their sizes are listed in the supplemental Table S1. The binding of the following eight proteins identified in the mass spectrometric analyses to RNA2 Δ1 was confirmed by using RNA affinity chromatography of RNA2 Δ1 followed by Western blotting: KSRP (K homology-type splicing regulatory protein), FUBP1, PTBP1 (polypyrimidine tract-binding protein 1), heterogeneous nuclear ribonucleoprotein D (hnRNPD), DHX9 (DEAH Box Helicase 9), U2AF65 (U2 Auxiliary Factor 65 kDa), vimentin, and β-actin (data not shown). Interestingly, we also observed the binding of damage-specific cleaved forms of some of these proteins, including FUBP1, PTBP1, and U2AF65 to RNA2 Δ1 in cisplatinum-treated nuclear extracts (Fig. 3*B* and data not shown) (48, 49).

FUBP1 Binds Intron 11 of the MDM2 Minigene—The differentially binding factor that migrated at ~65 kDa (Fig. 3*A*) and bound RNA2 Δ1 specifically in the extracts from cisplatinum-treated cells was identified as FUBP1 in the mass spectrometric analysis. FUBP1 is a single strand nucleic acid-binding helicase with a well documented role as the transcriptional enhancer of

c-*MYC* expression (31, 32). Its direct and specific binding to RNA2 Δ1 was confirmed by immunoblotting analyses following RNA affinity chromatography of RNA2 Δ1 and Δ3 in nuclear extracts of normal and damage-treated cells (Fig. 3*B*). Although the FUBP1 form that bound RNA2 Δ1 in normal nuclear extract migrated at the expected size of ~70 kDa, the damage-specific short form of FUBP1 that bound RNA2 Δ1 only in nuclear extract from damage-treated cells migrated at 65 kDa (Fig. 3*B*). To confirm that the presence of the short form of FUBP1 in the nuclear extract from damage-treated cells was not due to the fractionation technique employed, we examined FUBP1 protein in the whole cell, nuclear, and cytoplasmic extracts from untreated and cisplatinum-treated HeLa S3 cells (75 μM, 12 h). We observed the presence of the short form of FUBP1 in all three fractions of the cisplatinum-treated cells but not in the untreated cells (Fig. 3*C*), indicating that the appearance of the short form of FUBP1 is not artifactual. In addition, we tested the possibility that the differentially migrating form of FUBP1 seen in nuclear extract from damage-treated cells could be due to differential phosphorylation of FUBP1. We treated normal and damaged HeLa S3 nuclear extracts with calf intestinal phosphatase (CIP) to remove phosphate moieties from the phosphoproteins in the extracts and then performed Western blotting analysis for FUBP1. We observed no differences in the migration of the two forms of FUBP1 in nuclear extract from damage-treated cells between CIP-treated and -untreated samples. Similarly, full-length FUBP1 in normal nuclear extract did not respond to CIP treatment (Fig. 3*D*). As a positive control to gauge the efficiency of the phosphatase treatment of our extracts, we probed for SFRS1, a known phosphoprotein. Indeed, SFRS1 showed differential migration in nuclear extracts from both normal and damage-treated cells that were treated with CIP when compared with untreated extracts (Fig. 3*D*). These results indicate that the differential migration of the two forms of FUBP1 in nuclear extract from damage-treated cells is independent of phosphorylation.

A short form of FUBP1 has previously been described by Jang *et al.* (45) as a caspase 3 or caspase 7 cleavage product resulting from treatment with another DNA-damaging agent, etoposide. This form (Δ74), representing the C-terminal fragment obtained after cleavage of the full-length FUBP1 protein, migrated at approximately the same size (~65 kDa) as the short form of FUBP1 that we observed under cisplatinum treatment. To test the possibility that the damage-specific form that we observed is the result of caspase cleavage of full-length FUBP1 in cisplatinum-treated cells, we treated HeLa S3 cells with the pan-caspase inhibitor BAF (50 μM) or DMSO followed by 12 h of treatment with 75 μM cisplatinum. We observed that the short form of FUBP1 was generated in cisplatinum-treated HeLa S3 cells preconditioned with DMSO. However, the presence of the caspase inhibitor BAF prevented the generation of the short form of FUBP1, indicating that this form is indeed a product of caspase activity (Fig. 3*E*).

FUBP1 Enhances the Splicing Efficiency of the MDM2 3-11-12 Minigene in Normal Nuclear Extract in Vitro—As we observed the differential binding of FUBP1 to intron 11 of the *MDM2* minigene under normal and damaged conditions, we wanted to test the possibility that FUBP1 regulates alternative splicing of the *MDM2* minigene. To this end, we used an immunointerference *in vitro* splicing approach in which nuclear extracts were incubated with an antibody (H-42 clone; epitope mapping near the N terminus corresponding to amino acids 65–106) that recognized both the full-length and Δ74 forms of FUBP1 or corresponding isotype control. The nuclear extracts were then used to perform splicing reactions on the *MDM2* 3-11-12 minigene as described previously (22). The splicing efficiency was quantified as the ratio of the band intensity of full-length spliced (*3.11.12*) or the exon 11 skipped (*3.12*) products to the intensity of unspliced transcripts in each reaction (ImageQuant version 8.1). The change in the splicing efficiency was normalized to the isotype control within each experiment (Fig. 4*B*). Strikingly, we observed that immunointerference of FUBP1 in normal nuclear extracts resulted in a significant decrease in splicing efficiency of the *MDM2* minigene compared with the isotype control (Fig. 4*A*). There was no significant change in the ratio of skipped (*3.12*) to full-length (*3.11.12*) spliced products between the FUBP1-immunointerfered and isotype control reactions (Fig. 4*B*). Additionally, we tested the efficacy of another N-terminal FUBP1 antibody (N15 clone, recognizes only the full-length form of FUBP1 in Western blotting) in this assay but observed no changes in splicing (splicing efficiency or the ratio of skipped to full-length products) of the *MDM2* minigene compared with the corresponding isotype controls (data not shown). This limitation raises the possibility of the inadequacy of the N-15 clone to block the FUBP1 active site or conversely nonspecific effects of the H-42 clone. To address this, we subsequently employed siRNA-based techniques to accurately characterize the role of FUBP1 in *MDM2* splicing (see below). Additionally, to assess transcript specificity of FUBP1-mediated splicing regulation, we examined the splicing of a non-damage-responsive *p53* 7-8-9 minigene (22) using immunointerference. However, this minigene displayed very poor splicing capability in nuclear extracts containing either IgG or FUBP1 antibodies, and its splicing patterns could not be quantitated or evaluated. We were therefore unable to rule out FUBP1's role as a general splicing enhancer in these experiments.

FUBP1 Facilitates Efficient Splicing of Both the Upstream and Downstream Introns in MDM2 2-Exon Minigenes in Vitro—As we observed a decrease in splicing efficiency of the *MDM2* 3-11-12 minigene upon interference of FUBP1 in normal nuclear extracts (Fig. 4), we wanted to examine whether splicing of the upstream and downstream introns (relative to exon 11 in the 3-exon minigene) was affected by FUBP1. To test this, we created 2-exon minigenes 3–11 and 11–12 from the *MDM2* 3-11-12 minigene. We additionally created a 2-exon *p53* minigene (*p53* 8-9) to assess transcript specificity for FUBP1-mediated effects on splicing. We observed that splicing of the 11-12 minigene, which contains intron 11 with the FUBP1-binding sites, decreased in a statistically significant manner in FUBP1 immunointerference in normal nuclear extracts (Fig. 5*A*). This change was quantified as the ratio of band volumes of the spliced 11.12 products to the corresponding unspliced transcripts in each reaction (Fig. 5*B*). The change in the splicing efficiency was normalized to the rIgG isotype control within each experiment. Surprisingly, we observed that FUBP1 immunointerference led to a statistically significant decrease in splic-

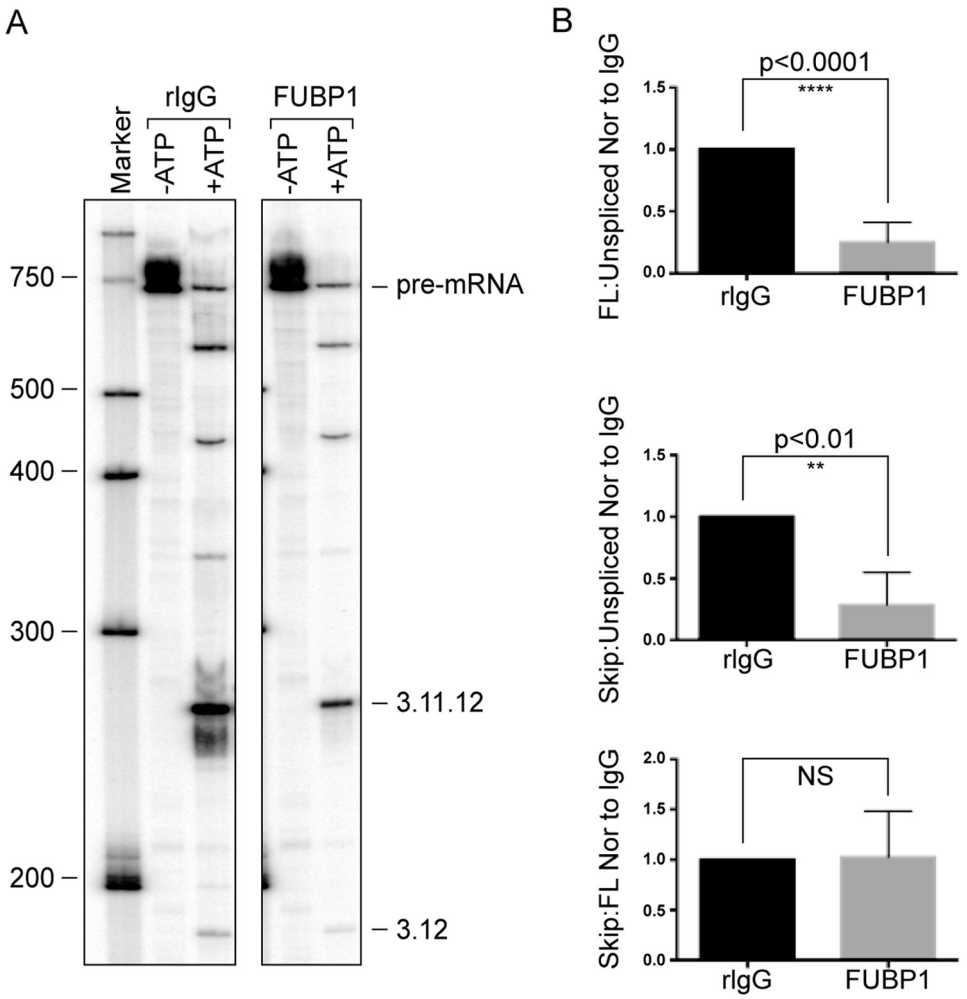

FIGURE 4. **Immunointerference of FUBP1 compromises the splicing efficiency of the *MDM2* 3-11-12 minigene.** *A,* immunointerference of FUBP1 (H-42 clone) that recognizes both full-length and short form of FUBP1, in normal nuclear extracts, results in a decrease in splicing efficiency of the *MDM2 3-11-12* minigene as seen in the decreased intensity of the spliced products 3.11.12 and 3.12 in comparison with the isotype control. *B,* splicing efficiency was quantified (ImageQuant version 8.1) as the ratio of pixel intensity of the 3.11.12 or 3.12 spliced products to unspliced pre-mRNA. These ratios were normalized to the rIgG isotype control and are graphically presented with S.E. (*error bars*). Two-tailed Student's *t* test indicates significant changes in splicing efficiency under FUBP1 immunointerference. However, no significant changes were observed in the ratio of skipped (3.12) to full-length (3.11.12) spliced product between the rIgG and FUBP1 immunointerference. *NS* is non-significant, $p > 0.5$ in the statistical analyses. **, $p < 0.01$; ****, $p < 0.0001$.

ing of the 3-11 *MDM2* minigene also, raising the possibility that FUBP1 can also bind and regulate the splicing of regions in the intron upstream of the damage-regulated exon 11. Moreover, we were able to show that this effect is transcript-specific because splicing of the *p53 8-9* minigene did not show a significant change upon interference with FUBP1 or rIgG treatment in the nuclear extracts (Fig. 5, *A* and *B*). To further confirm the transcript-specific effect of FUBP1-mediated splicing, we generated a 2-exon minigene *7-8* comprising the upstream intron of the *p53* 7-8-9 minigene and examined its splicing under FUBP1 or rIgG immunointerference conditions. As a positive control for these experiments, we used the *MDM2* 3-11 minigene construct whose splicing is decreased when FUBP1 activity is inhibited (Fig. 5, *A* and *B*). As expected, the 3-11 minigene showed a statistically significant decrease in splicing efficiency under FUBP1 immunointerference conditions when compared with rIgG control (Fig. 5, *C* and *D*). However, the splicing of the *p53* 7-8 minigene remained unchanged between both conditions (Fig. 5, *C* and *D*). This indicates that splicing of neither intron of the *p53 7-8-9* minigene is regulated by FUBP1.

FUBP1 Shows Differential Binding to the Upstream Intron—As the inactivation of FUBP1 in normal nuclear extracts significantly decreased the *in vitro* splicing of the 3-11 *MDM2* 2-exon minigene, we examined regions in the chimeric intron upstream of exon 11 in the *3-11-12 MDM2* minigene (intron 3/10) for FUBP1-binding sites. To this end, we used the UV cross-linking assay as described previously and examined the differential binding of factors between nuclear extracts from normal and damage-treated cells on radioactively labeled transcripts, RNAs A and B, which span the intron 3/10 (Fig. 6, *A* and *B*). RNA A showed the differential binding of the 65-kDa factor similar to RNA2 (Fig. 6*B*). We then used the RNA affinity chromatography technique to isolate the differential factors binding RNA A in nuclear extracts from normal and cisplatinum-damaged cells (Fig. 6*C*). Mass spectrometric analysis revealed the 65-kDa factor to be FUBP1, and furthermore, we confirmed the binding of FUBP1 to RNA A within the upstream intron by RNA affinity chromatography followed by western blotting (Fig. 6*D*) (anti-FUBP1 H-42 clone). This indicates that FUBP1 may regulate the splicing of the *MDM2* minigene through bind-

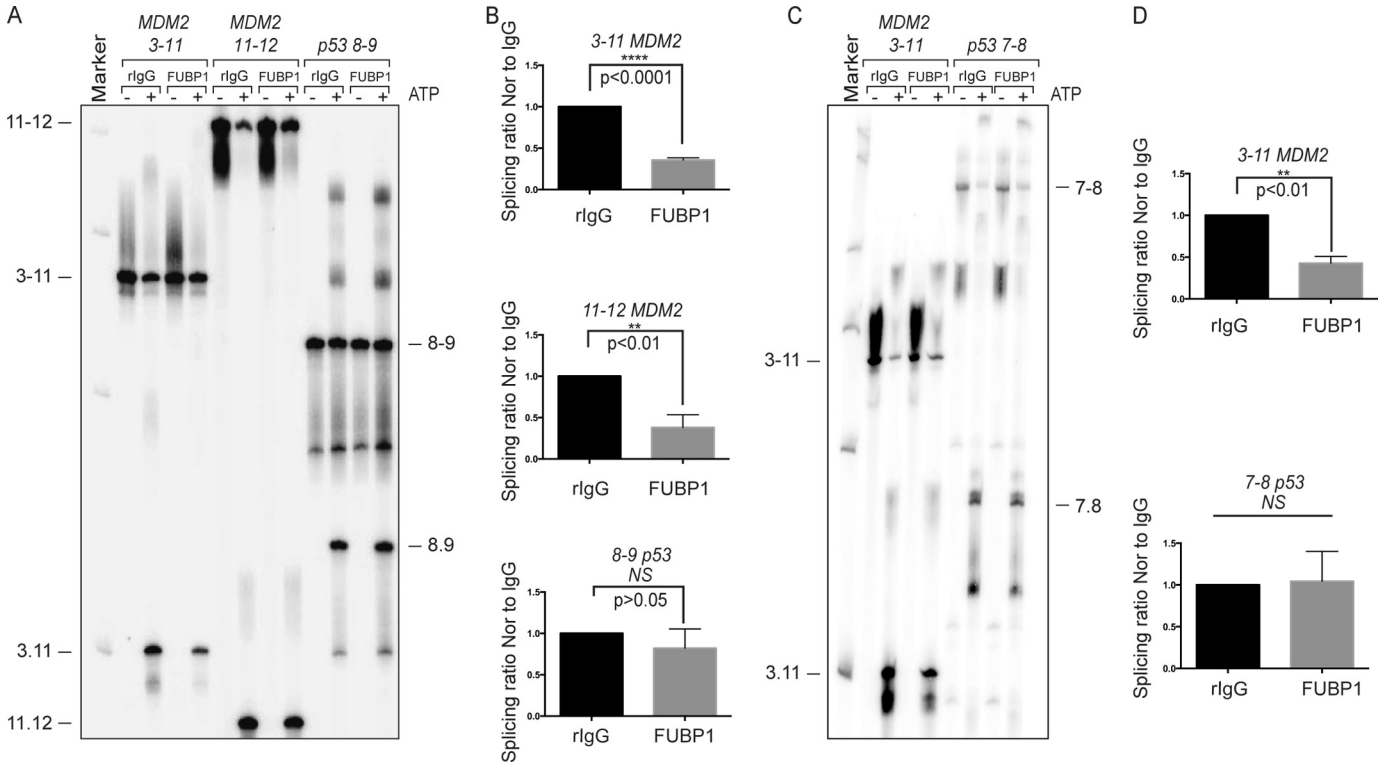

FIGURE 5. **FUBP1 immunointerference decreases splicing of both introns of the *MDM2* minigene but not the *p53* minigene indicating transcript specificity.** *A,* immunointerference with anti-FUBP1 (H-42 clone sc-48821 (lot number A1707) or rIgG isotype control was performed in normal nuclear extracts, which were then used in *in vitro* splicing of 2-exon minigenes derived from the *MDM2 3-11-12* minigene that spans either the intron upstream of exon 11 (*3–11* minigene, $n = 3$) or the intron downstream of exon 11 (*11–12* minigene, $n = 4$). The splicing of a 2-exon minigene (*8–9*) derived from a non-damage-responsive *p53* minigene (22) was also assayed under similar conditions ($n = 5$). The splicing of *3–11* and *11–12 MDM2* minigenes decreased significantly but not of the *8–9 p53* minigene. *B,* splicing of the minigenes was quantified (ImageQuant version 8.1) as the ratio of pixel intensity of the 3.11 or 11.12 or 8.9 spliced products to unspliced pre-mRNA. These ratios were normalized to the rIgG isotype control, and results from at least three independent experiments for each construct are graphically presented with S.E. (*error bars*). Two-tailed Student's *t* test indicates statistically significant changes in splicing efficiency under FUBP1 immunointerference for the *MDM2*-derived minigenes but not the *p53*-derived *8-9* minigene. *C,* splicing of *7-8* 2-exon construct derived from the *p53* minigene (upstream intron in the *p53 7-8-9* 3-exon minigene) was also examined in comparison with the *3-11 MDM2* minigene under conditions of FUBP1 immunointerference using the batch of H-42 FUBP1 antibody (lot number H3013). Shown here is a representative gel from three independent experiments. *D,* splicing of these minigenes was quantified as described above and represented graphically with S.E. (*error bars*). Two-tailed Student's *t* test indicates statistically significant changes in splicing efficiency under FUBP1 immunointerference for the *3-11 MDM2*-derived minigene but not the *p53*-derived *7-8* minigene. **, $p < 0.01$; ****, $p < 0.0001$. *NS* is non-significant, $p > 0.5$ in the statistical analyses.

ing sites on introns upstream and also downstream of the internal exon 11.

Our immunointerference results suggest that full-length FUBP1 is required in normal nuclear extracts for efficient splicing of the *MDM2* (2-exon and 3-exon) minigenes. We therefore wanted to test whether or not the damage-specific Δ74 form of FUBP1 contributes to *MDM2-ALT1* splicing in nuclear extracts from damage-treated cells (which express the Δ74 FUBP1 isoform at high levels) using an immunointerference approach in which the H-42 antibody blocks activity of both full-length and Δ74 FUBP1. However, the immunointerference *in vitro* splicing assay proved to be limiting for this purpose. This is because neither the 3-exon *MDM2* nor the 2-exon *MDM2* and *p53* minigene systems showed quantifiable splicing in these extracts in the presence of any IgG molecule due to the diminished splicing efficiency. We were therefore unable to accurately assess the role of the Δ74 FUBP1 form in the splicing of the *MDM2* and the p53 minigenes *in vitro*. Hence, in subsequent experiments, we used overexpression assays in cultured cells to examine the function of the Δ74 FUBP1 form in the context of *MDM2* splicing.

FUBP1 Overexpression Suppresses Damage-inducible Alternative Splicing of MDM2 Minigene—Because FUBP1 immunointerference decreased the splicing efficiency of the *MDM2* minigene *in vitro*, we wanted to test the effects of the overexpression of FUBP1 on the splicing of the *MDM2* minigene in cells under normal and damaged conditions. To do this, we overexpressed FUBP1 or a negative control (LacZ- or GFP-expressing plasmids) along with a stress-responsive *MDM2* minigene in HeLa cells. This stress-responsive *MDM2* minigene comprises exons 3, 4, and 10–12 and importantly retains the complete intron 11 (22), and it enabled us to assess the role of FUBP1 in the context of the native intron 11. Additionally, we assayed in a similar manner the function of the Δ74 short form of FUBP1 and caspase cleavage site mutant FUBP1 (AQPA) in which the caspase cleavage site (DQPD) has been mutated to prevent formation of the Δ74 form (45).

We hypothesized that FUBP1 overexpression would act as a positive regulator of minigene splicing even under damage. However, the damage-specific Δ74 form would act in a dominant negative manner and induce exon skipping in the minigene even in absence of damage. Indeed, the overexpression of

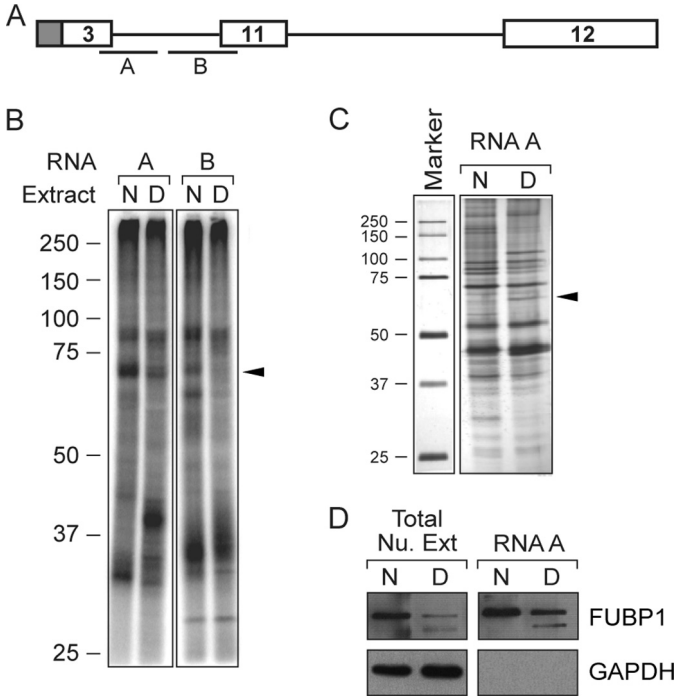

FIGURE 6. **FUBP1 binds the intron upstream of exon 11.** *A,* RNA A and B were designed to span the intron upstream of exon 11 of the *MDM2 3-11-12* minigene. *B,* RNAs A and B were subjected to the UVC cross-linking assay similar to the experiments performed in Fig. 1. RNA A showed differential cross-linking with the 65-kDa factor (*arrowhead*) between normal (*N*) and damage (*D*) conditions in a manner similar to RNA2. *C,* RNA affinity chromatography was performed on RNA A in nuclear extracts (*Nu. Ext*) from normal and cisplatinum-treated cells, and the differential band at 65 kDa (*arrowhead*) in the damage nuclear extract was isolated (silver-staining following SDS-PAGE) and sequenced using tandem mass spectrometry. The protein factor binding RNA A was identified as FUBP1. *D,* binding of FUBP1 to RNA A was confirmed by Western blotting (H-42 antibody) following RNA affinity chromatography.

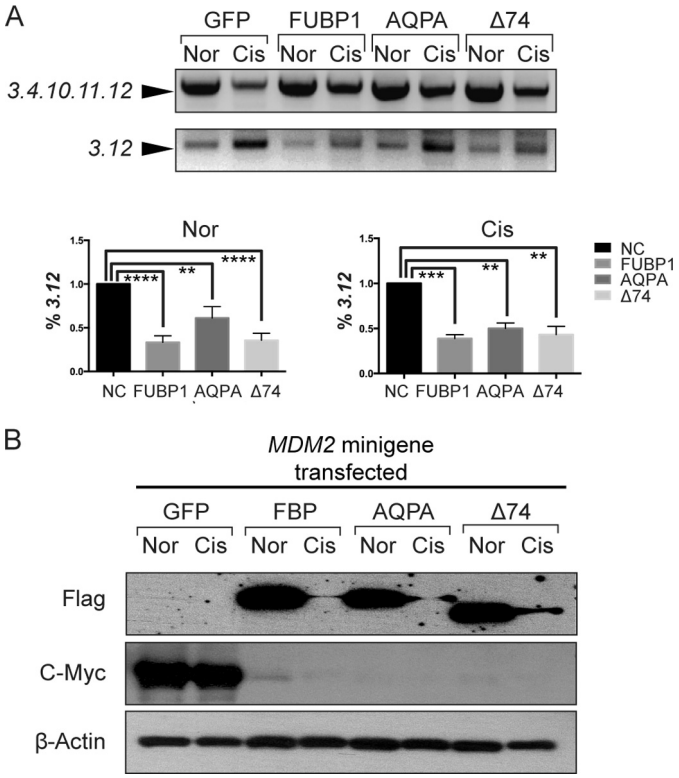

FIGURE 7. **Overexpression of FUBP1 and the Δ74 form suppresses the formation of *MDM2-ALT1* from an *MDM2* minigene upon cisplatinum treatment.** *A,* full-length FUBP1, the shorter isoform Δ74, a noncleavable form of FUBP1 (AQPA), or a negative control (MYC-tagged LacZ or GFP) were overexpressed in HeLa cells along with an *MDM2 3-4-10-11-12* minigene followed by no treatment (*Nor*) or 24 h of cisplatinum (*Cis*) treatment. RT-PCR was used to assess the splicing of the minigene. Shown here are the representative RT-PCR results for an experiment in which MYC-tagged GFP was used as negative control. The contrast of the panel showing the *3.12* skipped product was increased for better visualization purposes only. The relative quantification of the full-length and *3.12* spliced products was performed prior to this adjustment. The full-length *3.4.10.11.12* and the skipped *3.12* product intensities were assessed using ImageQuant version 8.1. The percentage of skipped product was determined as the internal band-intensity ratio of skipped to full-length products. The percent skipped (*3.12*) product under normal or cisplatinum treatment for all samples was then normalized to the corresponding negative control (*NC*). One-way analysis of variance with Dunnett's multiple comparisons test (GraphPad Prism 6.0c) was then used to determine the significance in the changes in *3.12* splicing between the negative control and the overexpression of the different isoforms of FUBP1 under untreated (*Nor*) or cisplatinum-treated (*Cis*) conditions. Full-length FUBP1 or its isoforms when overexpressed resulted in a statistically significant decrease in the formation of the *3.12* skipped products both under normal and damage conditions compared with the negative control (*NC*). These changes in splicing of the minigene are represented graphically as the percent *3.12* product under the various conditions. *Error bars* represent S.E. from three independent experiments. *B,* Western blotting was used to confirm overexpression of FUBP1 (FLAG), its various isoforms, and the negative control (MYC-tagged GFP is shown here). β-Actin was used as loading control. **, $p < 0.01$; ***, $p < 0.001$; ****, $p < 0.0001$.

FUBP1 and also the caspase cleavage mutant FUBP1 (AQPA) decreased the induction of *MDM2-ALT1* (3.12) upon cisplatinum treatment in a statistically significant manner when compared with overexpression of the negative control in these cells under both normal and damage conditions (Fig. 7*A*). Surprisingly, we found that the stress-specific Δ74 form of FUBP1 acted in a manner similar to full-length FUBP1 in that its overexpression also caused a statistically significant decrease in *MDM2-ALT1* induction under normal and damage conditions (Fig. 7*A*). Immunoblotting was used to confirm the overexpression of the FUBP1 proteins and the negative control (Fig. 7*B*).

Knockdown of FUBP1 Induces MDM2 Alternative Splicing Even in the Absence of Stress—As the overexpression of FUBP1 attenuated the induction of *MDM2-ALT1* from the minigene under cisplatinum stress, we reasoned that the knockdown of FUBP1 would have the opposite effect on *MDM2* splicing. To this end, we examined the splicing of endogenous *MDM2* in HeLa cells in the context of siRNA-mediated FUBP1 knockdown. Notably, the use of siRNA targeting *FUBP1* resulted in the knockdown of all forms of FUBP1 (both full-length and the damage-specific Δ74 forms). This is because these forms are derived from the same *FUBP1* pre-mRNA transcripts, and the Δ74 form is the result of the damage-induced, post-translational caspase-mediated cleavage of full-length FUBP1. Indeed, we observed that the knockdown of FUBP1 resulted in the induction of *MDM2-ALT1* splicing even under normal conditions, although the nonspecific siRNA-treated cells showed only full-length *MDM2* splicing under normal conditions (Fig. 8; compare *lane 3* with the control in *lane 1*). Moreover, cisplatinum stress in combination with the knockdown of FUBP1 resulted in a further increase in *MDM2-ALT1* splicing compared with cisplatinum treatment of cells transfected with the nonspecific siRNA (Fig. 8; compare *lane 2* to *lane 4*). The change in the cisplatinum-treated cells was not statistically significant, possibly due to saturation of the system. These results

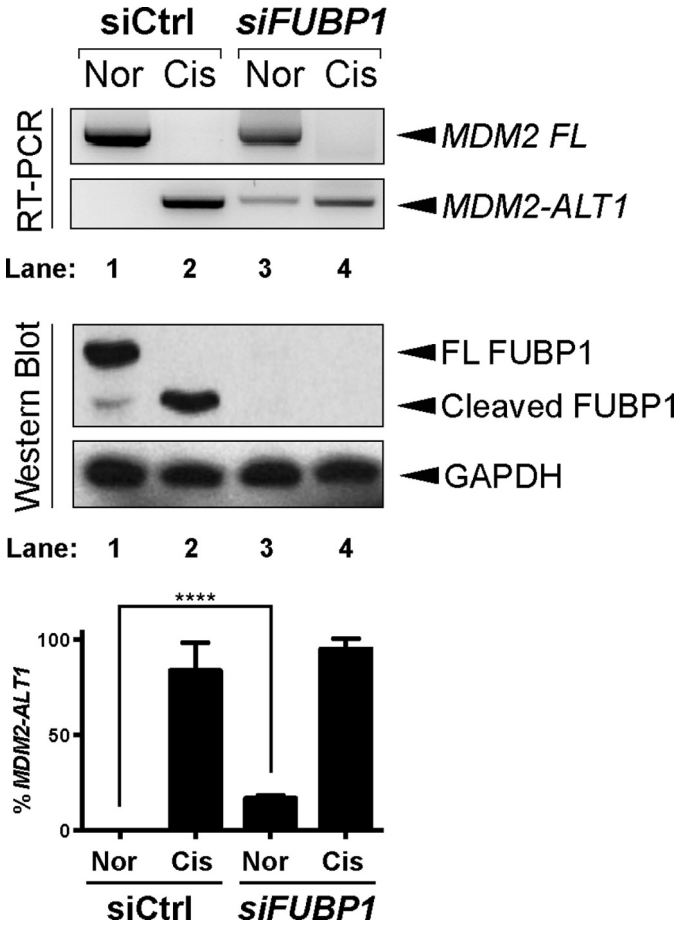

FIGURE 8. **Knockdown of FUBP1 results in the formation of *MDM2-ALT1* even under normal conditions.** HeLa cells were transfected with siRNA targeting FUBP1 (*siFUBP1*) or a nonspecific control siRNA (*siCtrl*) and then grown normally (*Nor*) or treated with cisplatinum (*Cis*) for 24 h and then harvested for total RNA and protein. Reverse transcription was performed followed by nested PCR to assess the splicing of endogenous *MDM2*. Knockdown of FUBP1 significantly increased *MDM2-ALT1* splicing in the absence of damage (compare *lane 3* to control *lane 1*). The knockdown of endogenous FUBP1 protein (both full-length and the cleaved Δ74 form) was confirmed using Western blotting (H-42), and GAPDH was used as loading control. The intensity of the *MDM2 FL* and *MDM2-ALT1* spliced products was quantified using ImageQuant version 8.1, and the ratio of skipped to full-length products was calculated as percent *MDM2-ALT1*. The results of three independent trials are represented graphically with S.E. (*error bars*). Student's *t* test (two-tailed, GraphPad Prism 6.0c) was used to assess the significance of the change in percent *MDM2-ALT1* between siCtrl and siFUBP1. ****, $p < 0.0001$.

indicate that loss of FUBP1 causes a decrease in the full-length *MDM2* transcript and a corresponding increase in the alternatively spliced form, supporting FUBP1's role as a positive regulator of *MDM2* splicing.

Alterations in the FUBP1 Gene Are a Feature of Several Malignancies—To examine whether or not FUBP1 expression was altered in other cancer types, we queried The Cancer Genome Atlas (TCGA) data portal maintained by the Memorial Sloan-Kettering Cancer Center or the cBioPortal (46, 47). When *FUBP1* expression was queried, the portal revealed alterations in *FUBP1* gene due to mutations, amplification, or deletions in 44 of the 69 published and unpublished cancer data sets maintained by the cBioportal. We have highlighted these alterations in *FUBP1* for the top 15 hits in our search of the portal (Fig. 9*A*). Consistent with the results observed by Bettegowda *et al.* (29), in oligodendrogliomas, the TCGA Brain lower grade glioma study (which includes oligodendrogliomas) appeared among the cancer types showing the highest frequency of mutations in *FUBP1* (9% of cases presented with mutations in *FUBP1*, Fig. 9*A*, *lane 2*). Moreover, these mutations were predicted to result in loss of FUBP1 expression or its inactivation in these tumors. We then examined the Kaplan-Meier survival estimates for the cancer studies for which these data were available, including the low grade glioma group. Interestingly, the glioma cohort did not show any changes in survival estimates between the patients with *FUBP1* alterations and those with wild-type *FUBP1* (Fig. 9*B*). Of all the other cancer types examined, only the lung adenocarcinoma (TCGA provisional study: *lane 8* in Fig. 9*A*) patients with alterations in *FUBP1* (5 of 129 cases) showed significantly decreased survival compared with patients with wild-type FUBP1 (log rank test $p = 0.02$, Fig. 9*B*).

DISCUSSION

The key finding in this study is the role of the oncogenic factor FUBP1 in the regulation of *MDM2* splicing. FUBP1 is single strand DNA and RNA-binding protein best known for its role as a transcriptional regulator of the proto-oncogene c-*MYC* in many cancer types (31, 32, 50, 51) and also as regulator of post-transcriptional events such as translation (38) and mRNA stability (23). However, despite the fact that FUBP1 has been isolated in association with spliceosomal complexes (40) and includes four K homology domains (domains homologous to heterogeneous nuclear ribonucleoprotein K, a component of the spliceosomal H complexes (52)), its role in splicing regulation has remained speculative until recently. Li *et al.* (41) showed that FUBP1 suppresses *triadin* exon 10 splicing in the context of a chimeric reporter minigene through its binding of a 30-nt AU-rich exonic splicing silencer element in this exon at a consensus sequence AUAUAUGAU. Our study, in contrast, shows that FUBP1 functions as an enhancer of splicing in the context of the oncogene *MDM2*. Using an *MDM2 3-11-12* minigene (22), we have identified the binding of FUBP1 to intronic splicing regulatory elements, ~120 nt in length, in intron 11 and intron 3/10 of this minigene (described in Singh *et al.* (22)) that are enriched in AU sequences. Although we could not identify a single consensus binding site described by Li *et al.* (41) for FUBP1 in these elements, it is possible that it can bind multiple, closely related AU-rich sequences to enhance splicing of the internal exon 11 of the *MDM2* minigene.

Possible Mechanisms for FUBP1-mediated Splicing of MDM2—The inactivation of FUBP1 *in vitro* compromised the splicing of the introns of the *MDM2* minigene resulting in accumulation of unspliced RNA. In cultured cells, when FUBP1 was knocked down, this was reflected in the skipping of exons of the endogenous *MDM2* gene yielding *MDM2-ALT1* transcripts even under normal conditions. This event is possibly a result of compromised splicing efficiency resulting from the knockdown of FUBP1. I*n vitro*, when transcription was uncoupled from splicing, we observed that FUBP1 inactivation resulted in a decrease in splicing efficiency of the *MDM2* minigene. In this case, it is possible that FUBP1 aids in recruiting the spliceosomal machinery to the splice sites of the *MDM2* minigene by

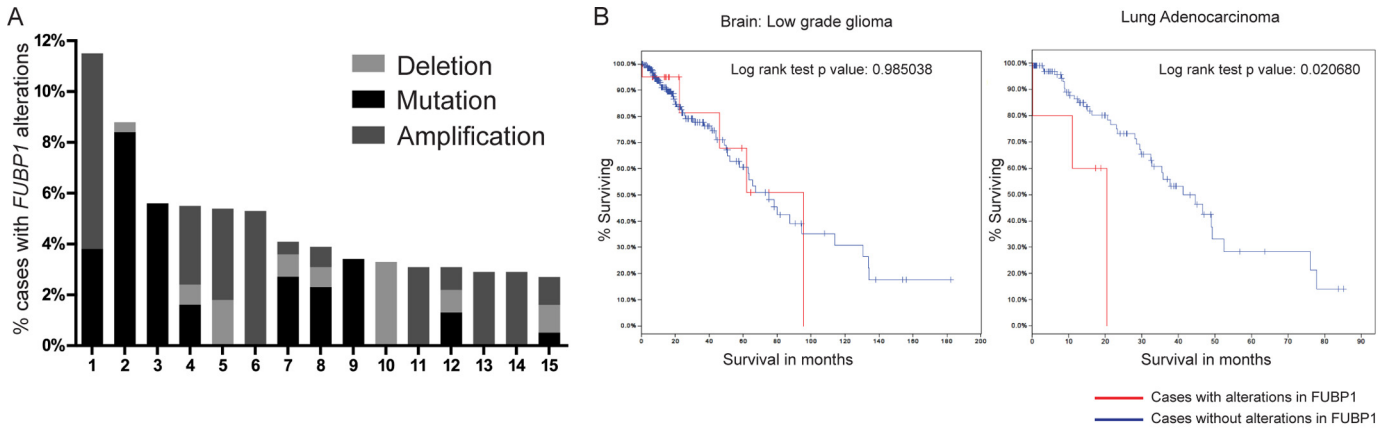

#	Study Name	# of cases altered
1	Bladder Urothelial Carcinoma (TCGA, Provisional)	3 of 26
2	Brain Lower Grade Glioma (TCGA, Provisional)	23 of 262
3	Colorectal Adenocarcinoma (Genentech, Nature 2012)	4 of 72
4	Bladder Urothelial Carcinoma (TCGA, Nature 2014)	7 of 127
5	Prostate Adenocarcinoma (Broad/Cornell, Cell 2013)	3 of 56
6	Sarcoma (MSKCC/Broad, Nature Genetics 2010)	11 of 207
7	Stomach Adenocarcinoma (TCGA, Provisional)	9 of 219
8	Lung Adenocarcinoma (TCGA, Provisional)	5 of 129
9	Small Cell Lung Cancer (CLCGP, Nature Genetics 2012)	1 of 29
10	Prostate Adenocarcinoma (TCGA, Provisional)	8 of 244
11	Sarcoma (TCGA, Provisional)	4 of 127
12	Lung Adenocarcinoma (TCGA, Nature, in press)	7 of 230
13	Uterine Corpus Endometrial Carcinoma (TCGA, Provisional)	7 of 240
14	Uterine Corpus Endometrioid Carcinoma (TCGA, Nature 2013)	7 of 240
15	Lung Adenocarcinoma (Broad, Cell 2012)	5 of 182

Brain: Low grade glioma	#total cases	#cases deceased	median months survival
Cases with Alterations in FUBP1	23	5	95.51
Cases without Alterations in FUBP1	218	50	75.11

Lung Adenocarcinoma	#total cases	#cases deceased	median months survival
Cases with Alterations in FUBP1	5	3	20.47
Cases without Alterations in FUBP1	111	36	41.30

FIGURE 9. ***FUBP1* gene alterations are observed across several cancer types in The Cancer Genome Atlas.** The TCGA was queried for *FUBP1* mutations and copy number alterations across 69 cancer studies archived in the TCGA via the cBioPortal. *A,* plot represents the percentage of cases with *FUBP1* alterations (gene amplification, mutations, deletions, or multiple alterations) in the top 15 hits (cancer studies). The *table* below the plot provides an explanation of the study presented and the number of cases in the study with *FUBP1* alterations. *B,* Kaplan-Meier survival estimate curve for low grade gliomas (*A, lane 2*) shows no change in survival between patients with altered *FUBP1* (*red line*) and those with wild-type *FUBP1* (*blue line*). However, the Kaplan-Meier survival estimate curve for lung adenocarcinoma (*A, lane 8*) shows significant change in survival between patients with altered *FUBP1* and those with wild-type *FUBP1* ($p = 0.02$).

binding to intronic splicing enhancer elements. Adding a layer of support to this possibility is the fact that FUBP1 has been shown to interact with PUF60 (poly(U)-binding factor 60), a splicing factor that interacts with U2AF65 and facilitates recruitment of U2 small nuclear ribonucleoproteins (53, 54). However, the interaction of PUF60 and FUBP1 has only been shown to occur in the context of c-*MYC* transcription regulation where a splice variant of PUF60, referred to as the FIR protein (FBP interacting repressor, lacking the first 17 amino acids of PUF60), interacts with and antagonizes FUBP1 in the transcriptional complex (55). The possibility that FUBP1 and PUF60 interact and function together in the context of splicing regulation has yet to be explored.

Another important finding in our study is that the inactivation of FUBP1 *in vitro* decreased the splicing of both the upstream and the downstream introns relative to exon 11 in the 3-11-12 *MDM2* minigene. Subsequently, we showed the binding of FUBP1 and its damage-specific cleaved form of FUBP1 to elements in both these introns. It is therefore possible that FUBP1 simultaneously binds both the introns across exon 11 to facilitate better recruitment of the spliceosome or positive regulatory factors while masking or competing with negative regulatory factors. Furthermore, we show that the effect of FUBP1 on splicing may be transcript-specific. This is because FUBP1 did not affect the splicing of either intron of the non-damage-responsive *p53* 7-8-9 minigene (22) in a statistically significant manner, although a slight decreasing trend was observed in the splicing of the *8-9* minigene upon FUBP1 immunointerference (Fig. 5, *A* and *B*).

FUBP1 Δ74 and Its Role in MDM2 Splicing—We used a stress-responsive *MDM2* minigene bearing an intact intron 11 to examine the roles of these forms of FUBP1 in *MDM2* splicing. As the full-length FUBP1 or the Δ74 isoform bound the minigene under normal or damaged conditions respectively, we had hypothesized opposing roles for these forms in the splicing of *MDM2*. Interestingly, both full-length and cleaved FUBP1 behaved in a similar fashion by suppressing the formation of *MDM2-ALT1* under stress thereby acting as positive regulators of *MDM2* splicing. However, this does not exclude the possibility that Δ74 could still function in an antagonistic manner to full-length FUBP1 under physiological conditions wherein the relative levels of these isoforms and their localization could be factors determining their functionality. Moreover, the negative splicing regulatory factors that actually facilitate the damage-induced skipping of *MDM2* exons have yet to be uncovered and may more easily negatively affect the Δ74 isoform. Candidates showing differential binding to the RNA2 region and/or other unidentified factors likely compete with FUBP1 under damage to bind the *cis* elements on *MDM2* and mediate its stress-induced alternative splicing.

In short, the regulation of efficient splicing of the *MDM2* pre-mRNA by FUBP1 (as indicated by the effects of its overexpression and knockdown in cells, Figs. 7 and 8) sets the stage for alterations in splicing patterns in response to specific stimuli, wherein mechanisms antagonistic to FUBP1 may function to alter the splicing efficiency of specific exons and create alternative splice forms of *MDM2*.

Role of FUBP1 in Cancer—FUBP1 itself is considered a proto-oncogene due to its role in the etiology of several types of cancer where it is overexpressed (23–28). However, a small subset of oligodendrogliomas (a common brain malignancy) with "loss of function" mutations in *FUBP1* has been identified where FUBP1 is considered a tumor suppressor (28–30). Regardless of the role it plays, FUBP1 is an important modifier of crucial tumor-suppressive and oncogenic programs within the cell. In this respect, it has been shown to function through both c-*MYC*-dependent and -independent pathways as a regulator of transcriptional and post-transcriptional events such as pre-mRNA translation (23, 25, 36, 38, 50, 51, 56, 57). For instance, FUBP1 has inextricable ties with the p53 tumor-suppressor pathway through its transcriptional control of far upstream element-containing genes c-*MYC* and *USP29* and also via its regulation of translation and stability of nucleophosmin and *p21* mRNA (23, 38, 56, 57). Additionally, the complex interactions of the various targets of FUBP1 among themselves or with other factors in the p53 pathway make FUBP1 an important player in this tumor-suppressor pathway (58, 59). In that light, an important aspect of our study is that we have characterized the oncogene *MDM2* as a substrate of FUBP1-mediated splicing. The role of FUBP1 as a regulator of *MDM2* splicing can have important ramifications for the MDM2-p53 axis. Now, with our evidence pointing toward its role as a modulator of *MDM2* splicing, a direct mode of involvement of FUBP1 in the complex p53 pathway has emerged.

When we examined The Cancer Genome Atlas via the cBioPortal for the impact of aberrations in FUBP1 expression on patient survival in various cancer types, we observed that only a low frequency of alterations in *FUBP1* gene has been observed across several cancer types (Fig. 9*A*). Many of the mutations reported are predicted to result in loss of FUBP1 expression. However, upon mining the information via this portal, we observed no significant changes in patient survival due to the presence of *FUBP1* gene alterations in most cancer types, including low grade gliomas. Only in the TCGA provisional lung adenocarcinoma study in which 3% of the cases presented with altered *FUBP1* was a statistically significant survival decrease observed in patients with mutated or altered *FUBP1*. Additionally, the studies queried via the cBioPortal do not account for FUBP1 expression changes at the mRNA and protein levels. For instance, the hepatocellular carcinoma cohorts queried in this manner show only about 0.6% of cases with mutations or gene amplifications. However, FUBP1 has been shown to be overexpressed in liver carcinoma (23). Hence, more intricate mining of the raw data for FUBP1 expression changes will bring out the impact of FUBP1 on cancer prognosis or progression in a better manner. Overall, these results indicate that FUBP1 over- or under-expression is significant over several cancer types. However, whether altered FUBP1 expression affects its functions in pre-mRNA splicing or transcription or post-transcriptional processing is open for exploration. We have shown that FUBP1 enhances the splicing efficiency of *FL-MDM2* and could therefore serve to additionally enhance the expression and activity of FL-MDM2 in those cancer types where its overexpression mediates the tumorigenic phenotype. As *MDM2* is subject to multiple splicing events in response to a variety of stresses, the ability of FUBP1 to improve splicing efficiency also poses FUBP1 as a target for modifications that promote negative regulation of *MDM2* splicing. The factors, which play into the negative aspects of *MDM2* splicing regulation, have yet to be characterized. Indeed, UV cross-linking and RNA affinity chromatography revealed the differential binding of several other factors and their damage-specific isoforms to the *MDM2* minigene in the nuclear extracts from damage-treated cells (Figs. 1–3 and 6 and supplemental Table S1). It is conceivable that these factors, through complex interactions with the spliceosome or other regulatory factors, contribute to the damage-induced *MDM2-ALT1* splicing and therefore demand further characterization.

In summary, our study has uncovered a mechanism for the regulation of *MDM2* gene expression via splicing control by FUBP1, a finding that opens up an additional avenue for exploring targets for cancer therapeutics that modulate the MDM2-p53 tumor-suppressor axis.

Acknowledgments—We express our gratitude to Dr. Sharon Dent (MD Anderson Cancer Center, Houston, TX) for the kind gift of the plasmid expressing FUBP1 cDNA. We also thank Dr. Katsumi Kitagawa (Nationwide Children's Hospital Research Institute, Columbus, OH) for the caspase inhibitor BAF and also the members of his laboratory for technical support. We also thank Lisa Feurer for assistance in figure preparation. We also extend our gratitude to Dr. Will Ray and Rajeswari Swaminathan for their intellectual input in the TCGA data-mining experiments. Additionally, we thank other members of the Chandler laboratory for their technical and intellectual support.

REFERENCES

1. Honda, R., Tanaka, H., and Yasuda, H. (1997) Oncoprotein MDM2 is a ubiquitin ligase E3 for tumor suppressor p53. *FEBS Lett.* **420,** 25–27
2. Oliner, J. D., Pietenpol, J. A., Thiagalingam, S., Gyuris, J., Kinzler, K. W., and Vogelstein, B. (1993) Oncoprotein MDM2 conceals the activation domain of tumour suppressor p53. *Nature* **362,** 857–860
3. Momand, J., Zambetti, G. P., Olson, D. C., George, D., and Levine, A. J. (1992) The mdm-2 oncogene product forms a complex with the p53 protein and inhibits p53-mediated transactivation. *Cell* **69,** 1237–1245
4. Fakharzadeh, S. S., Trusko, S. P., and George, D. L. (1991) Tumorigenic potential associated with enhanced expression of a gene that is amplified in a mouse tumor cell line. *EMBO J.* **10,** 1565–1569
5. Momand, J., Jung, D., Wilczynski, S., and Niland, J. (1998) The MDM2 gene amplification database. *Nucleic Acids Res.* **26,** 3453–3459
6. Bartel, F., Taylor, A. C., Taubert, H., and Harris, L. C. (2001) Novel mdm2 splice variants identified in pediatric rhabdomyosarcoma tumors and cell lines. *Oncol. Res.* **12,** 451–457
7. Kraus, A., Neff, F., Behn, M., Schuermann, M., Muenkel, K., and Schlegel, J. (1999) Expression of alternatively spliced mdm2 transcripts correlates with stabilized wild-type p53 protein in human glioblastoma cells. *Int. J. Cancer* **80,** 930–934
8. Sigalas, I., Calvert, A. H., Anderson, J. J., Neal, D. E., and Lunec, J. (1996) Alternatively spliced mdm2 transcripts with loss of p53 binding domain sequences: transforming ability and frequent detection in human cancer. *Nat. Med.* **2,** 912–917
9. Sánchez-Aguilera, A., García, J. F., Sánchez-Beato, M., and Piris, M. A. (2006) Hodgkin's lymphoma cells express alternatively spliced forms of HDM2 with multiple effects on cell cycle control. *Oncogene* **25,** 2565–2574
10. Lukas, J., Gao, D. Q., Keshmeshian, M., Wen, W. H., Tsao-Wei, D., Rosenberg, S., and Press, M. F. (2001) Alternative and aberrant messenger RNA

splicing of the mdm2 oncogene in invasive breast cancer. *Cancer Res.* **61,** 3212–3219
11. Hori, M., Shimazaki, J., Inagawa, S., Itabashi, M., and Hori, M. (2000) Alternatively spliced MDM2 transcripts in human breast cancer in relation to tumor necrosis and lymph node involvement. *Pathol. Int.* **50,** 786–792
12. Evdokiou, A., Atkins, G. J., Bouralexis, S., Hay, S., Raggatt, L. J., Cowled, P. A., Graves, S. E., Clayer, M., and Findlay, D. M. (2001) Expression of alternatively-spliced MDM2 transcripts in giant cell tumours of bone. *Int. J. Oncol.* **19,** 625–632
13. Tamborini, E., Della Torre, G., Lavarino, C., Azzarelli, A., Carpinelli, P., Pierotti, M. A., and Pilotti, S. (2001) Analysis of the molecular species generated by MDM2 gene amplification in liposarcomas. *Int. J. Cancer* **92,** 790–796
14. Matsumoto, R., Tada, M., Nozaki, M., Zhang, C. L., Sawamura, Y., and Abe, H. (1998) Short alternative splice transcripts of the mdm2 oncogene correlate to malignancy in human astrocytic neoplasms. *Cancer Res.* **58,** 609–613
15. Jacob, A. G., O'Brien, D., Singh, R. K., Comiskey, D. F., Jr., Littleton, R. M., Mohammad, F., Gladman, J. T., Widmann, M. C., Jeyaraj, S. C., Bolinger, C., Anderson, J. R., Barkauskas, D. A., Boris-Lawrie, K., and Chandler, D. S. (2013) Stress-induced isoforms of MDM2 and MDM4 correlate with high-grade disease and an altered splicing network in pediatric rhabdomyosarcoma. *Neoplasia* **15,** 1049–1063
16. Steinman, H. A., Burstein, E., Lengner, C., Gosselin, J., Pihan, G., Duckett, C. S., and Jones, S. N. (2004) An alternative splice form of Mdm2 induces p53-independent cell growth and tumorigenesis. *J. Biol. Chem.* **279,** 4877–4886
17. Fridman, J. S., Hernando, E., Hemann, M. T., de Stanchina, E., Cordon-Cardo, C., and Lowe, S. W. (2003) Tumor promotion by Mdm2 splice variants unable to bind p53. *Cancer Res.* **63,** 5703–5706
18. Volk, E. L., Fan, L., Schuster, K., Rehg, J. E., and Harris, L. C. (2009) The MDM2–a splice variant of MDM2 alters transformation *in vitro* and the tumor spectrum in both Arf- and p53-null models of tumorigenesis. *Mol. Cancer Res.* **7,** 863–869
19. Zheng, T., Wang, J., Zhao, Y., Zhang, C., Lin, M., Wang, X., Yu, H., Liu, L., Feng, Z., and Hu, W. (2013) Spliced MDM2 isoforms promote mutant p53 accumulation and gain-of-function in tumorigenesis. *Nat. Commun.* **4,** 2996
20. Chandler, D. S., Singh, R. K., Caldwell, L. C., Bitler, J. L., and Lozano, G. (2006) Genotoxic stress induces coordinately regulated alternative splicing of the p53 modulators MDM2 and MDM4. *Cancer Res.* **66,** 9502–9508
21. Dias, C. S., Liu, Y., Yau, A., Westrick, L., and Evans, S. C. (2006) Regulation of hdm2 by stress-induced hdm2alt1 in tumor and nontumorigenic cell lines correlating with p53 stability. *Cancer Res.* **66,** 9467–9473
22. Singh, R. K., Tapia-Santos, A., Bebee, T. W., and Chandler, D. S. (2009) Conserved sequences in the final intron of MDM2 are essential for the regulation of alternative splicing of MDM2 in response to stress. *Exp. Cell Res.* **315,** 3419–3432
23. Rabenhorst, U., Beinoraviciute-Kellner, R., Brezniceanu, M. L., Joos, S., Devens, F., Lichter, P., Rieker, R. J., Trojan, J., Chung, H. J., Levens, D. L., and Zörnig, M. (2009) Overexpression of the far upstream element binding protein 1 in hepatocellular carcinoma is required for tumor growth. *Hepatology* **50,** 1121–1129
24. Malz, M., Weber, A., Singer, S., Riehmer, V., Bissinger, M., Riener, M. O., Longerich, T., Soll, C., Vogel, A., Angel, P., Schirmacher, P., and Breuhahn, K. (2009) Overexpression of far upstream element binding proteins: a mechanism regulating proliferation and migration in liver cancer cells. *Hepatology* **50,** 1130–1139
25. Singer, S., Malz, M., Herpel, E., Warth, A., Bissinger, M., Keith, M., Muley, T., Meister, M., Hoffmann, H., Penzel, R., Gdynia, G., Ehemann, V., Schnabel, P. A., Kuner, R., Huber, P., Schirmacher, P., and Breuhahn, K. (2009) Coordinated expression of stathmin family members by far upstream sequence element-binding protein-1 increases motility in non-small cell lung cancer. *Cancer Res.* **69,** 2234–2243
26. Ma, J., Chen, M., Xia, S. K., Shu, W., Guo, Y., Wang, Y. H., Xu, Y., Bai, X. M., Zhang, L., Zhang, H., Zhang, M., Wang, Y. P., and Leng, J. (2013) Prostaglandin E2 promotes liver cancer cell growth by the upregulation of FUSE-binding protein 1 expression. *Int. J. Oncol.* **42,** 1093–1104
27. Zhang, F., Tian, Q., and Wang, Y. (2013) Far upstream element-binding protein 1 (FUBP1) is overexpressed in human gastric cancer tissue compared to non-cancerous tissue. *Onkologie* **36,** 650–655
28. Baumgarten, P., Harter, P. N., Tönjes, M., Capper, D., Blank, A. E., Sahm, F., von Deimling, A., Kolluru, V., Schwamb, B., Rabenhorst, U., Starzetz, T., Kögel, D., Rieker, R. J., Plate, K. H., Ohgaki, H., Radlwimmer, B., Zörnig, M., and Mittelbronn, M. (2014) Loss of FUBP1 expression in gliomas predicts FUBP1 mutation and is associated with oligodendroglial differentiation, IDH1 mutation and 1p/19q loss of heterozygosity. *Neuropathol. Appl. Neurobiol.* **40,** 205–216
29. Bettegowda, C., Agrawal, N., Jiao, Y., Sausen, M., Wood, L. D., Hruban, R. H., Rodriguez, F. J., Cahill, D. P., McLendon, R., Riggins, G., Velculescu, V. E., Oba-Shinjo, S. M., Marie, S. K., Vogelstein, B., Bigner, D., Yan, H., Papadopoulos, N., and Kinzler, K. W. (2011) Mutations in CIC and FUBP1 contribute to human oligodendroglioma. *Science* **333,** 1453–1455
30. Sahm, F., Koelsche, C., Meyer, J., Pusch, S., Lindenberg, K., Mueller, W., Herold-Mende, C., von Deimling, A., and Hartmann, C. (2012) CIC and FUBP1 mutations in oligodendrogliomas, oligoastrocytomas and astrocytomas. *Acta Neuropathol.* **123,** 853–860
31. Vindigni, A., Ochem, A., Triolo, G., and Falaschi, A. (2001) Identification of human DNA helicase V with the far upstream element-binding protein. *Nucleic Acids Res.* **29,** 1061–1067
32. Duncan, R., Bazar, L., Michelotti, G., Tomonaga, T., Krutzsch, H., Avigan, M., and Levens, D. (1994) A sequence-specific, single-strand binding protein activates the far upstream element of c-myc and defines a new DNA-binding motif. *Genes Dev.* **8,** 465–480
33. Braddock, D. T., Louis, J. M., Baber, J. L., Levens, D., and Clore, G. M. (2002) Structure and dynamics of KH domains from FBP bound to single-stranded DNA. *Nature* **415,** 1051–1056
34. Benjamin, L. R., Chung, H. J., Sanford, S., Kouzine, F., Liu, J., and Levens, D. (2008) Hierarchical mechanisms build the DNA-binding specificity of FUSE binding protein. *Proc. Natl. Acad. Sci. U.S.A.* **105,** 18296–18301
35. Chien, H. L., Liao, C. L., and Lin, Y. L. (2011) FUSE binding protein 1 interacts with untranslated regions of Japanese encephalitis virus RNA and negatively regulates viral replication. *J. Virol.* **85,** 4698–4706
36. Zheng, Y., and Miskimins, W. K. (2011) Far upstream element binding protein 1 activates translation of p27Kip1 mRNA through its internal ribosomal entry site. *Int. J. Biochem. Cell Biol.* **43,** 1641–1648
37. Huang, P. N., Lin, J. Y., Locker, N., Kung, Y. A., Hung, C. T., Lin, J. Y., Huang, H. I., Li, M. L., and Shih, S. R. (2011) Far upstream element binding protein 1 binds the internal ribosomal entry site of enterovirus 71 and enhances viral translation and viral growth. *Nucleic Acids Res.* **39,** 9633–9648
38. Olanich, M. E., Moss, B. L., Piwnica-Worms, D., Townsend, R. R., and Weber, J. D. (2011) Identification of FUSE-binding protein 1 as a regulatory mRNA-binding protein that represses nucleophosmin translation. *Oncogene* **30,** 77–86
39. Min, H., Turck, C. W., Nikolic, J. M., and Black, D. L. (1997) A new regulatory protein, KSRP, mediates exon inclusion through an intronic splicing enhancer. *Genes Dev.* **11,** 1023–1036
40. Rappsilber, J., Ryder, U., Lamond, A. I., and Mann, M. (2002) Large-scale proteomic analysis of the human spliceosome. *Genome Res.* **12,** 1231–1245
41. Li, H., Wang, Z., Zhou, X., Cheng, Y., Xie, Z., Manley, J. L., and Feng, Y. (2013) Far upstream element-binding protein 1 and RNA secondary structure both mediate second-step splicing repression. *Proc. Natl. Acad. Sci. U.S.A.* **110,** E2687–2695
42. Mayeda, A., and Krainer, A. R. (1999) Preparation of HeLa cell nuclear and cytosolic S100 extracts for *in vitro* splicing. *Methods Mol. Biol* **118,** 309–314
43. Zhu, H., Hasman, R. A., Young, K. M., Kedersha, N. L., and Lou, H. (2003) U1 snRNP-dependent function of TIAR in the regulation of alternative RNA processing of the human calcitonin/CGRP pre-mRNA. *Mol. Cell. Biol.* **23,** 5959–5971
44. Wagner, E. J., and Garcia-Blanco, M. A. (2002) RNAi-mediated PTB depletion leads to enhanced exon definition. *Mol. Cell* **10,** 943–949

45. Jang, M., Park, B. C., Kang, S., Chi, S. W., Cho, S., Chung, S. J., Lee, S. C., Bae, K. H., and Park, S. G. (2009) Far upstream element-binding protein-1, a novel caspase substrate, acts as a cross-talker between apoptosis and the c-myc oncogene. *Oncogene* **28,** 1529–1536
46. Cerami, E., Gao, J., Dogrusoz, U., Gross, B. E., Sumer, S. O., Aksoy, B. A., Jacobsen, A., Byrne, C. J., Heuer, M. L., Larsson, E., Antipin, Y., Reva, B., Goldberg, A. P., Sander, C., and Schultz, N. (2012) The cBio cancer genomics portal: an open platform for exploring multidimensional cancer genomics data. *Cancer Discov.* **2,** 401–404
47. Gao, J., Aksoy, B. A., Dogrusoz, U., Dresdner, G., Gross, B., Sumer, S. O., Sun, Y., Jacobsen, A., Sinha, R., Larsson, E., Cerami, E., Sander, C., and Schultz, N. (2013) Integrative analysis of complex cancer genomics and clinical profiles using the cBioPortal. *Sci. Signal.* **6,** pl1
48. Back, S. H., Shin, S., and Jang, S. K. (2002) Polypyrimidine tract-binding proteins are cleaved by caspase-3 during apoptosis. *J. Biol. Chem.* **277,** 27200–27209
49. Izquierdo, J. M. (2008) Fas splicing regulation during early apoptosis is linked to caspase-mediated cleavage of U2AF65. *Mol. Biol. Cell* **19,** 3299–3307
50. Weber, A., Kristiansen, I., Johannsen, M., Oelrich, B., Scholmann, K., Gunia, S., May, M., Meyer, H. A., Behnke, S., Moch, H., and Kristiansen, G. (2008) The FUSE binding proteins FBP1 and FBP3 are potential c-myc regulators in renal but not in prostate and bladder cancer. *BMC Cancer* **8,** 369
51. Ding, Z., Liu, X., Liu, Y., Zhang, J., Huang, X., Yang, X., Yao, L., Cui, G., and Wang, D. (2013) Expression of far upstream element (FUSE) binding protein 1 in human glioma is correlated with c-Myc and cell proliferation. *Mol. Carcinog.* 10.1002/mc.22114
52. Zhou, Z., Licklider, L. J., Gygi, S. P., and Reed, R. (2002) Comprehensive proteomic analysis of the human spliceosome. *Nature* **419,** 182–185
53. Hastings, M. L., Allemand, E., Duelli, D. M., Myers, M. P., and Krainer, A. R. (2007) Control of pre-mRNA splicing by the general splicing factors PUF60 and U2AF(65). *PLoS One* **2,** e538
54. Page-McCaw, P. S., Amonlirdviman, K., and Sharp, P. A. (1999) PUF60: a novel U2AF65-related splicing activity. *RNA* **5,** 1548–1560
55. Liu, J., He, L., Collins, I., Ge, H., Libutti, D., Li, J., Egly, J. M., and Levens, D. (2000) The FBP interacting repressor targets TFIIH to inhibit activated transcription. *Mol. Cell* **5,** 331–341
56. Liu, J., Chung, H. J., Vogt, M., Jin, Y., Malide, D., He, L., Dundr, M., and Levens, D. (2011) JTV1 co-activates FBP to induce USP29 transcription and stabilize p53 in response to oxidative stress. *EMBO J.* **30,** 846–858
57. Atanassov, B. S., and Dent, S. Y. (2011) USP22 regulates cell proliferation by deubiquitinating the transcriptional regulator FBP1. *EMBO Rep.* **12,** 924–930
58. Xiao, J., Zhang, Z., Chen, G. G., Zhang, M., Ding, Y., Fu, J., Li, M., and Yun, J. P. (2009) Nucleophosmin/B23 interacts with p21WAF1/CIP1 and contributes to its stability. *Cell Cycle* **8,** 889–895
59. Colombo, E., Bonetti, P., Lazzerini Denchi, E., Martinelli, P., Zamponi, R., Marine, J. C., Helin, K., Falini, B., and Pelicci, P. G. (2005) Nucleophosmin is required for DNA integrity and p19Arf protein stability. *Mol. Cell. Biol.* **25,** 8874–8886